5. Processing Algorithms

Note: Optional dual polarization processing algorithms are described in Appendix B.

This chapter describes the processing algorithms implemented within the RVP8 signal processor. The discussion is confined to the mathematical description of these algorithms. Figure 5–1 shows the overall process by which the RVP8 converts the IF signal into corrected reflectivity, velocity, and width. Table 5–1 summarizes the quantities that are measured and computed by the RVP8. The type of the quantity (i.e., real or complex) is also given. Subscripts are sometimes used to denote successive samples in time from a given range bin. For example, s_n denotes the "I" and "Q" time series or "video" sample from the n'th pulse from a given range bin. In cases where it is obvious, the subscripts denoting the pulse (time) are dropped. The descriptions of all the data processing algorithms are phrased in terms of the operations performed on data from a single range bin- identical processing then being applied to all of the selected ranges. Thus, there is no need to include a range subscript in this data notation.

It is frequently convenient to combine two simultaneous samples of "I" and "Q" into a single complex number (called a phaser) of the form:

$$s = I + jQ$$

where "j" is the square root of –1. Most of the algorithms presented in this chapter are defined in terms of the operations performed on the "s"'s, rather than the "I"'s and "Q"'s. The use of the complex terms leads to a more concise mathematical expression of the signal processing techniques being used. In actual operation, the complex arithmetic is simply broken down into its real-valued component parts in order to be computed by the RVP8 hardware. For example, the complex product:

$$s = W \times Y$$

is computed as

$$\begin{aligned} Real\{s\} &= Real\{W\}\ Real\{Y\} \ - \ Imag\{W\}\ Imag\{Y\} \\ Imag\{s\} &= Real\{W\}\ Imag\{Y\} \ + \ Imag\{W\}\ Real\{Y\} \end{aligned}$$

where "Real{}" and "Imag{}" represent the real and imaginary parts of their complex-valued argument. Note that all of the expanded computations are themselves real-valued.

In addition to the usual operations of addition, subtraction, division, and multiplication of complex numbers, we employ three additional unary operators: "||", "Arg" and "*". Given a number "s" in the complex plane, the magnitude (or modulus) of s is equal to the length of the vector joining the origin with "s", i.e. by Pythagoras:

$$|s| = \sqrt{Real\{s\}^2 + Imag\{s\}^2}$$

The signed (CCW positive) angle made between the positive real axis and the above vector is:

$$\measuredangle = Arg\{s\} = \arctan\left[\frac{Imag\{s\}}{Real\{s\}}\right]$$

where this angle lies between $-\pi$ and $+\pi$ and the signs of Real{s} and Imag {s} determine the proper quadrant. Note that this angle is real, and is uniquely defined as long as |s| is non-zero. When |s| is equal to zero, Arg{s} is undefined. Finally, the "complex conjugate" of "s" is that value obtained by negating the imaginary part of the number, i.e.,

$$s^* = Real\{s\} - j\ Imag\{s\}.$$

Note that Arg{s*} = –Arg{s}. The reader is referred to any introductory text on complex numbers for clarification of these points.

Table 5–1: Algebraic Quantities Within the RVP8 Processor

p	Instantaneous IF-receiver data sample	*Real*
b	Instantaneous Burst-pulse data sample	*Real*
I, Q	Instantaneous quadrature receiver components	*Real*
s	Instantaneous time series phaser value	*Complex*
s'	Time series after clutter filter	*Complex*
T_0	Zeroth lag autocorrelation of A values	*Real*
R_0	Zeroth lag autocorrelation of A' values	*Real*
R_1	First lag autocorrelation of A' values	*Complex*
R_2	Second lag autocorrelation of A' values	*Complex*
SQI	Signal Quality Index	*Real*
V	Mean velocity	*Real*
W	Spectrum Width	*Real*
CCOR	Clutter correction	*Real*
LOG	Signal to noise ratio for thresholding	*Real*
SIG	Signal power of weather	*Real*
C	Clutter power	*Real*
N	Noise power	*Real*
Z	Corrected Reflectivity factor	*Real*
T	UnCorrected Reflectivity factor	*Real*

The following sections cover the various parts of the diagram shown in Figure 5–1, i.e.,

- IF Signal Processing
- I/Q processing and clutter filtering
- Range averaging and clutter microsuppression
- Moment calculations (reflectivity, velocity, spectrum width)
- Thresholding for data quality and Speckle Filtering
- Reflectivity Calibration
- Special algorithms for ambiguity resolution (dual PRF, dual PRT, Random Phase)
- Calibration and Testing

Figure 5–1: Flow Diagram of RVP8 Processing

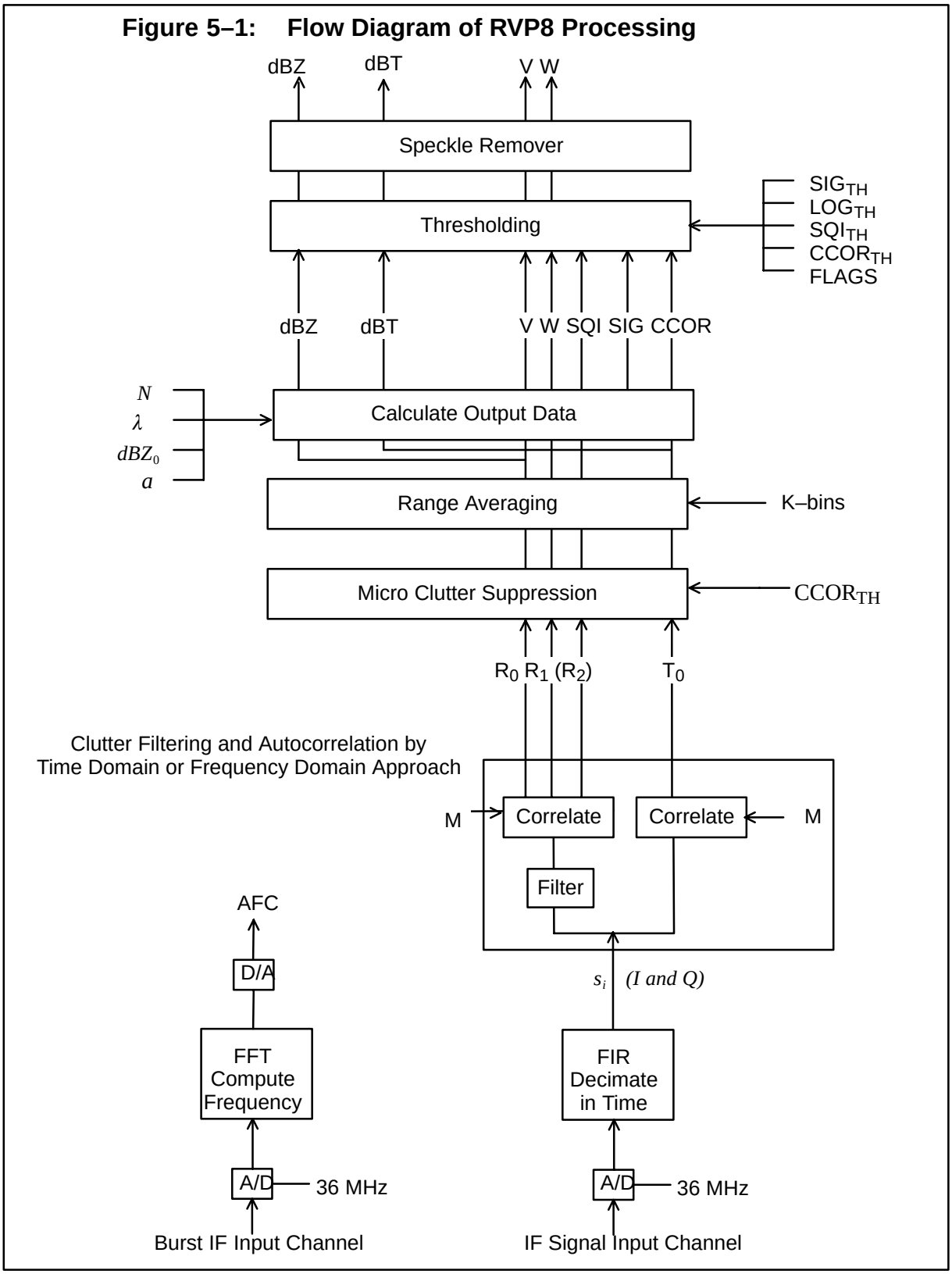

5.1 IF Signal Processing

The starting point for all computations within the RVP8 are the instantaneous IF-receiver samples p_n and, the instantaneous burst-pulse or COHO reference samples b_n. These data are available at a very high sampling rate (typically 36MHz), which makes possible the digital implementation of functions that are traditionally performed by discrete components in an analog receiver. The RVP8's all-digital approach replaces a great deal of analog hardware, avoids problems of aging and maintenance, and makes it easy to tune-up the receiver and alter its parameters.

This section describes these IF signal processing steps. Please refer to Figure 1-3 for a block diagram of the IF processing that is performed.

5.1.1 FIR (Matched) Filter

The RVP8 implements a digital version of the "matched" filter that is found in the traditional analog radar receiver. The equivalent Finite-Impulse-Response (FIR) filter is designed using an interactive graphical procedure described in Section 4.4. The filter length (number of taps), center frequency, and bandwidth are all adjustable. The design procedure computes two sets of filter coefficients ${f^i}_n$ and ${f^q}_n$ such that the instantaneous quadrature samples at a given bin are:

$$I = \sum_{n=0}^{N-1} {f^i}_n \times p_n, \qquad Q = \sum_{n=0}^{N-1} {f^q}_n \times p_n$$

where N is the length of the filter. The input samples p_n are centered on the range bin to which the (I, Q) pair is assigned. Note that some of the p_n are likely to overlap among adjacent bins, i.e., the filter length may be chosen to be greater than the bin spacing. Such an overlap introduces a slight correlation between successive bins, but the longer length allows a better filter to be designed.

The sums above for I and Q are computed on the RVP8/Rx board using dedicated FIR chips (for revisions A and B) that can perform up to 576 million sums of products per second. The Rev C RVP8/Rx uses a more flexible FPGA. The p_n are represented as 16-bit signed integers, and the ${f^i}_n$ and ${f^q}_n$ are represented as 10-bit (Rev.A/B) or 16-bit (Rev.C) signed integers. A numerical optimization procedure is used to quantize the ideal filter coefficients into their hardware values. The overall spectral purity of the FIR filter will typically be greater than 66dBc (Rev.A/B) and 84dBc (Rev.C).

The reference phase for each transmitted pulse is computed using the same two FIR sums, except with b_n substituted for the p_n. For a magnetron system the N b_n samples are centered on the transmitted burst; for a Klystron system they may be obtained from the burst pulse (recommended) or from the CW COHO. If the Klystron is phase modulated by an external phase shifter (as opposed to the RVP8/Tx digital transmitter board), then the samples should be from the modulated COHO.

The ${f^i}_n$ coefficients are computed as:

$${f^i}_n \;=\; l_n \times \sin\left[\frac{\pi}{4} + 2\pi \frac{f_{IF}}{f_{SAMP}}\left(n - \frac{N-1}{2}\right)\right] \quad , \quad n = 0 \ldots N-1$$

where f_{IF} is the radar intermediate frequency, f_{SAMP} is the RVP8/IFD crystal sampling frequency, and l_n are the coefficients of an N-point symmetric low-pass FIR filter that is matched to the bandwidth of the transmitted pulse. The multiplication of the l_n terms by the *sin()* terms effectively converts to the low-pass filter to a band-pass filter centered at the radar IF. The formula for the $f^q{}_n$ coefficients is identical except that *sin()* is replaced with *cos()*.

The phase of the sinusoid terms, and the symmetry of the l_n terms, has been carefully chosen to have a valuable overall symmetry property when *n* is replaced with *(N–1)–n*, i.e., the sequence is reversed:

$$f^i{}_{(N-1)-n} = l_{(N-1)-n} \times \sin\left[\frac{\pi}{4} + 2\pi \frac{f_{IF}}{f_{SAMP}}\left(((N-1)-n) - \frac{N-1}{2}\right)\right]$$

$$f^i{}_{(N-1)-n} = l_n \times \cos\left[\frac{\pi}{4} + 2\pi \frac{f_{IF}}{f_{SAMP}}\left(n - \frac{N-1}{2}\right)\right]$$

$$f^i{}_{(N-1)-n} = f^q{}_n$$

Thus, the coefficients needed to compute *I* are merely the reversal of the coefficients needed to compute *Q*; if you know $f^i{}_n$, then you also know $f^q{}_n$.

5.1.2 RVP8/Rx Receiver Modes

The RVP8 supports six fundamental IFD and RVP8/Rx configurations which allow you to choose the best style of IF processing for your particular site. The following table summarizes the options where, ***BW*** is the net IF sampling rate (full 72MHz, or halfband filtered 36MHz), ***DynR*** is the dynamic range (normal single channel, or extra wide dual channel), ***Pol*** is the number of polarizations, ***Freq*** is the number of distinct intermediate frequencies, and ***IFD*** is the number of IFD's, along with their corresponding RVP8/Rx cards.

#	BW	DynR	Filt	Pol	Freq	IFD	Description
0	Full	Norm	Norm	1	1	1	Standard single channel
1	Full	Norm	Norm	2	2	1	Dual Pol on two frequencies
2	Full	Norm	Norm	2	1	2	Dual Pol on separate IFDs
3	Half	Norm	Norm	2	1	1	Dual Pol on single IFD
4	Half	Wide	Norm	1	1	1	Extra wide dynamic range
5	Half	Norm	Long	1	1	1	Extra long/fast FIR filters

The first three modes were already supported in the previous RVP7 processor. The last three modes are unique to the RVP8 and bring some exciting additional capabilities to the signal processor. The six receiver modes are summarized below. Please see the *Discussion of Halfband Filtering* (Section 5.1.2.1) as it applies to Modes 3-5, and the *Discussion of Wide Dynamic Range* (Section 5.1.2.2)for additional details on using Mode-4.

Mode-0: Standard Single Channel This is the most common "vanilla" mode that is used by single-polarization CW-pulsed radars whose front-end LNA has a dynamic range less than ≈92dB. The (I,Q) data are computed from IF samples at their full acquisition rate (32MHz for Rev.D IFDs, and 72MHz for Rev.F), and the resulting dynamic range from 14-bit IFD samples is well matched to the RF components.

Mode-1: Dual-Pol On Two Frequencies This was the original dual-Pol configuration used by the RVP7 several years ago. A single IFD A/D converter receives the "H" and "V" channels using two distinct intermediate frequencies. Two different STALOs are required in this configuration, making the RF/IF components a bit more expensive, but only one IFD is required.

Mode-2: Dual-Pol On Separate IFDs This mode was introduced into the RVP8 in 2003, and provides dual polarization data using two IFDs connected to two RVP8/Rx cards in the same PCI chassis. A single intermediate frequency is used, hence only one STALO is required.

Mode-3: Dual-Pol On Single IFD This is the recommended dual polarization mode for all new RVP8 installations. The "H" and "V" channels are fed into the Primary and Secondary IFD inputs using a single intermediate frequency. System cost and complexity are both optimized in this design since only a single IFD, RVP8/Rx card, and STALO are required to process both polarization channels.

Mode-4: Extra Wide Dynamic Range Radars having very high performance front-end LNAs can preserve the full benefit of that investment by running two separate IF signals into the Primary (HiGain) and Secondary (LoGain) IFD inputs. A nominal channel separation of 25–30dB might be used to achieve an overall dynamic range of up to 110dB.

Mode-5: Extra Long/Fast FIR Filters This mode is intended for pulse compression systems that require unusually long filters (up to 80µsec), or finer range resolution in order to employ higher compressed bandwidths without the risk of missing echoes between bins. For example, a 30µsec pulse could be processed at an incoming range resolution of 50 meters and then range averaged down to 150meter output spacing.

5.1.2.1 Discussion of Halfband Filtering Modes 3-5

Traditionally, the IFD used by the RVP7 and RVP8 has sent raw 14-bit A/D samples from its Burst and IF inputs directly to either the RVP7/Main or RVP8/Rx cards for FIR filtering and conversion into complex (I,Q) values. The IFD would function simply as a waveform sampling device (hence the acronym **IF D**igitizer), and all of the front-end signal processing took place downstream of it.

This model has changed with the introduction of the Rev.F IFD which has the ability to carry out several billion multiply-accumulate cycles per second. This means that IF samples from multiple signals can be preprocessed entirely within the IFD and then encoded without loss onto the fixed bandwidth of its digital downlink. The new receiver modes 3 through 5 rely on this hardware capability and use a method known as "Halfband Filtering" to effectively double the downlink data rate.

Section 2.2.7 of the *RVP8 User's Manual* contains a detailed account of how A/D quantization noise affects the dynamic range of the IFD. Briefly, for the Rev.F A/D converter which runs at 72MHz, the contribution of A/D quantization noise within any given 1MHz interval is 72 times smaller than the total noise of the converter itself. This is an important property of all wideband sampling systems: the noise floor after processing, and hence the dynamic range, are improved by increasing the fundamental A/D sampling rate.

Normally the IFD sends 72MHz A/D samples from a single input channel directly down to the RVP8/Rx PCI card. The samples are sent at full speed in order to realize maximum reduc-

tion of the final (I,Q) noise floor. But suppose we wanted to send two A/D waveforms down the same data link by interleaving the samples together. Each channel would have to be down-sampled to 36MHz in order to fit within this format, but that would cause its (I,Q) noise floor to increase by 3dB.

To avoid this, we do not create the 36MHz streams merely by discarding every other A/D sample, but rather, by passing the original 72MHz data through a halfband digital filter and then discarding every other point of this filtered A/D stream. The difference is important. Since the halfband filter has removed all of the A/D quantization noise from half of the original Nyquist interval, there will be no increase in noise density within the passband of the (I,Q) filter when the halfband stream is downsampled to 36MHz. Thus, the A/D noise that would normally have folded into the (I,Q) data at 36MHz is first removed by the halfband filter so that we're left with a 36MHz stream having *the same dynamic range* of the original 72MHz samples.

The IFD halfband filter is a 49-Tap equiripple FIR filter having 40dB of stopband rejection and 0.175dB of passband ripple. The passband extends either from 0–16.5MHz when configured as a lowpass filter, or 19.5–36MHz when configured for highpass. The RVP8 automatically selects the correct type of filter depending on the intermediate frequency specified in the **Mb** menu. The halfband filter has linear phase and is therefore non-dispersive. This means that it is totally suitable for handling compressed pulses and other wideband Tx/Rx waveforms.

5.1.2.2 Discussion of Wide Dynamic Range Mode-4

When a two channel IFD is used as an extended dynamic range receiver there are some important decisions to make with respect to setting up the RF/IF levels that drive the IFD.

The first of these is the amount of signal level separation between the high gain and the low gain IFD inputs. There is an absolute minimum and absolute maximum channel separation that still allows the IFD to capture the full dynamic range of the receiver. If a signal level separation is made that is outside of these absolute limits valuable receiver dynamic range will be lost.

- ***The absolute minimum separation*** of the channels is equal to the total dynamic range of the receiver minus the dynamic range of a single channel of the IFD. Generally, the total dynamic range of the receiver is set by the LNA. For example, if we are considering a 1μsec pulse (1MHz bandwidth), the dynamic range of the LNA may be about 105dB, and the dynamic range of a single channel of the IFD is about 84dB (from –78dBm to +6dBm). In this case, the minimum separation would be 21dB. At minimum separation, the overlap of the low gain channel and the high gain channel will be maximized, and that overlap is equal to the dynamic range of a signal channel of the IFD minus the separation. In this case, the overlap is (84dB – 21dB) = 63dB.
- ***The absolute maximum separation*** of the channels is simply the dynamic range of a single channel of the IFD. In the above example this would be 84dB. At

maximum separation, the overlap of the low gain channel and the high gain channel is zero -- we begin using one as soon as the other has begun to saturate.

We see that there can be a large difference between the absolute minimum and maximum signal level separations; thus additional criteria must be considered to choose an optimum value that is between these diverse limits.

Choosing a proper separation value is a tradeoff of several factors. If the separation value is too low, the IFDs may end up operating very close to their noise floors. And if the separation is too high, then the overlap between the two channels is reduced which makes it difficult for the IFD to make a smooth transition as it combines the data from both channels. Too high a separation may also result in receiver components that are not practical to build.

As a rule of thumb, channel separations in the 22–30dB range provide a good balance of the above criteria. In the case of a 1µsec pulse this results in an overlap interval of approximately 55-63dB, which is sufficient for good IFD transitions and also leads to receiver components that are practical to build.

Once a separation value has been chosen, one must consider how to build the receiver to achieve this. The basic receiver will take the form of an LNA and a mixer followed by a splitter resulting in a low gain channel and a high gain channel. We know the gain difference in the two channels (the separation value), but we must find the actual gain to use in each channel.

If we consider the total system dynamic range as generally set by the LNA (105dB in the above example), we can estimate the minimum detectable signal input to the LNA as well as the maximum usable linear level at the IFD. If the LNA has a noise figure of 1dB and we are using a 1µsec pulse, the minimum detectable signal at the LNA input is –113dBm, and thus the maximum signal is 105dB above this, or –8dBm. If we add to these number the gain of the LNA and the conversion loss of the mixer (and any other losses experienced through the power splitter for the low gain and high gain channels), we can use this information to determine the signal values of the components in these two channels.

For example, if the LNA has a gain of 17dB, the mixer has a conversion loss of 7dB, there is 1dB miscellaneous losses and 3dB loss in the power splitter, then the signal level at the output of the power splitter is (–113 + 18 – 7 – 1 – 3) = –106dBm for the minimum signal, and and –1dBm for the maximum signal. In the low gain channel, we need to bring the –1dBm up to the maximum input value of the IFD (+6dBm). To do this we need about 8dB of amplification (7dB plus one more deciBel to account for the anti–alias filter loss of the IFD). If we assume 25dB of channel separation, on the high gain channel we require about +33dB of amplification. Finally, this tells us that on the low gain channel, the minimum and maximum signals presented to the IFD are (–106 + 8) = –98dBm and (–1 + 8) = 7dBm. For the high gain channel, the signal levels are (–106 + 33) = –73dBm and (–1 + 33) = +32dBm. Note that as +32dBm is above the maximum input level tolerated by the IFD, the amplifier on the high gain channel must limit its output to less than +16dBm. Thus an amplifier with an output saturation value of between +10dBm and +15dBm should be used.

5.1.3 Automatic Frequency Control (AFC)

AFC is used on magnetron systems to tune the STALO to compensate for magnetron frequency drift. It is not required for Klystron systems. The STALO is typically tuned 30 or 60 MHz away from the magnetron frequency. The maximum tuning range of the AFC feedback is approximately 7MHz on each side of the center frequency. This is limited by the analog filters that are installed just before the signal and burst IF inputs on the IFD. It is important that the system's IF frequency is at least 4MHz away from any multiple of half the digital sampling frequency, i.e., 18, 36, 54, or 72MHz.

The RVP8 analyzes the burst pulse samples from each pulse, and produces a running estimate of the power-weighted center frequency of the transmitted waveform. This frequency estimate is the basis of the RVP8's AFC feedback loop, whose purpose is to maintain a fixed intermediate frequency from the radar receiver.

The instantaneous frequency estimate is computed using four autocorrelation lags from each set of $N\ b_n$ samples. This estimate is valid over the entire Nyquist interval (e.g., 18MHz to 36MHz), but becomes noisy within 10% of each end. Since the span of the burst pulse samples is only approximately one microsecond, several hundred estimates must be averaged together to get an estimate that is accurate to several kiloHertz. Thus, the AFC feedback loop will typically have a time constant of several seconds or more.

Most of the burst pulse analysis routines, including the AFC feedback loop, are inhibited from running immediately after making a pulsewidth change. The center-of-mass calculations are held off according to the value of *Settling time (to 1%) of burst frequency estimator*, and the AFC loop is held off by the *Wait time before applying AFC* (**Mb** Section 3.2.6). This prevents the introduction of transients into the burst analysis algorithms each time the pulsewidth changes.

Additional information about using AFC can be found in Sections 2.2.11, 2.4, and 3.2.6.

5.1.4 Burst Pulse Tracking

The RVP8 has the ability to track the power-weighted center-of-mass of the burst pulse, and to automatically shift the trigger timing so that the pulse remains in the center of the burst analysis window of the **Pb** plot. This means that external sources of drift in the timing of the transmitted pulse (temperature, aging, etc.) will be tracked and nulled out during normal operation; so that fixed targets will remain fixed in range, and clean Tx phase measurements will always be available on every pulse.

The Burst Pulse Tracker feedback loop makes changes to the trigger timing in response to the measured position of the burst. Timing changes will generally be made only when the RVP8 is not actively acquiring data, in the same way that AFC feedback is held off for similar "quiet" times. However, if the center-of-mass has drifted more than 1/3 the width of the burst analysis window, then the timing adjustment will be made right away. Also, there will be an approximately 5ms interruption in the normal trigger sequence whenever any timing changes are made.

The Burst Pulse Tracker and AFC feedback loop are each fine-tuning servos that keep the burst pulse "centered" in time and frequency. These servos have been expanded to include a combined "Hunt Mode" that will track down a missing burst pulse when we are uncertain of both its time and frequency. This coarse-tuning mode is especially valuable for initializing the two fine-tuning servos in radar systems that drift significantly with time and temperature.

When the radar transmitter is *On* but the burst pulse is missing, it may be because either of the following have happened:

- It is misplaced in time, i.e., the Tx pulse is outside of the window displayed in the **Pb** plotting command. In this case, the trigger timing needs to be changed in order to bring the center of the pulse back to the center of the window.
- It is mistuned in frequency, i.e., the AFC feedback is incorrect and has caused the burst frequency to fall outside of the passband of the RVP8 anti-alias filters. In this case the AFC (or DAFC) needs to be changed so that proper tuning is restored.

The Hunt Mode performs a 2-dimensional search in time and frequency to locate the burst; searching across a $\pm$20μsec time window, and across the entire AFC span. If a valid Tx pulse (i.e., meeting the minimum power requirement) can be found anywhere within those intervals then the Burst Pulse Tracker and AFC loops will be initialized with the time and frequency values that were discovered. The fine servos then commence running with a good burst signal starting from those initial points.

Depending on how the hunting process has been configured in the **Mb** menu, the whole procedure may take several seconds to complete. The RVP8's host computer interface remains completely functional during this time, but any acquired data would certainly be questionable. GPARM status bits in word #55 indicate when the hunt procedure is running, and whether it has completed successfully. The BPHUNT (Section 6.26) opcode allows the host computer to initiate Hunt Mode when it knows or can sense that a burst pulse should be present

5.1.5 Interference Filter

The interference filter is an optional processing step that can be applied to the raw *(I,Q)* samples that emerge from the FIR filter chips. The intention of the filter is to remove strong but sporadic interfering signals that are occasionally received from nearby man-made sources. The technique relies on the statistics of such interference being noticeably different from that of weather.

For each range bin at which *(I,Q)* data are available, the interference filter algorithm uses the received power (in deciBels) from the three most recent pulses:

$$P_{n-2},\ P_{n-1},\ \text{and}\ P_n$$

where:

$$P_n \ = \ 10\log_{10}\left(I_n^2 + Q_n^2\right) .$$

If the three pulse powers have the property that:

$$\left| P_{n-1} - P_{n-2} \right| < C_1 \quad \text{and} \quad \left| P_n - P_{n-1} \right| > C_2 \qquad \text{(Alg.1)}$$

then (I_n, Q_n) is replaced by (I_{n-1}, Q_{n-1}). Here C_1 and C_2 are constants that can be tuned by the user to match the type of interference that is anticipated, and the error rates that can be tolerated. For certain environments it may be the case that good results can be obtained with $C_1 = C_2$; but the RVP8 does not force that restriction.

This 3-pulse algorithm is only intended to remove interference that arrives on isolated pulses, and for which there are at least two clear pulses in between. Interference that tends to arrive in bursts will not be rejected.

Two variations on the fundamental algorithm are also defined. The CFGINTF command (Section 6.23) allows you to choose which of these algorithms to use, and to tune the two threshold constants. You may also do this directly from the **Mp** setup menu (Section 3.2.2).

$$| P_{n-1} - P_{n-2} | < C_1 \quad \text{and} \quad P_n - P_{n-1} > C_2 \qquad \text{(Alg.2)}$$

$$| P_{n-1} - P_{n-2} | < C_1 \quad \text{and} \quad P_n - \mathit{LinAvg}(P_{n-1}, P_{n-2}) > C_2 \qquad \text{(Alg.3)}$$

Where *LinAvg()* denotes the deciBel value of the linear average of the two deciBel powers. The Alg.2 and Alg.3 algorithms also include the receiver noise level(s) as part of their decision criteria. Whenever power levels are intercompared in the algorithms, any power that is less than the noise level is first set equal to that noise level. This makes the filters much more robust and properly tunable, so that interference is more successfully rejected on top of blank receiver noise.

Optimum values for C_1 and C_2 will vary from site to site, but some guidance can be obtained using numerical simulations. The results shown below were obtained when the algorithms were applied to realistic weather time series having a spectrum width = 0.1 (Nyquist), SNR = +10dB, and an intermittent additive interference signal that was 16dB stronger than the weather. The interference arrived in isolated single pulses with a probability of 2%.

Performance of the three algorithms is summarized in the first three columns of Table 5–2, for which C_1 and C_2 have the common value shown. The fourth column also uses Algorithm #3, but with the value of C_1 raised by 2dB. The "Missed" rate is defined as the percentage of interference points that manage to get through the filtering process without being removed. The "False" (false alarm) rate is the percentage of non-interference points that are incorrectly modified when they should have been left alone.

Table 5–2: Algorithm Results for +16dB Interference

	Alg.1		Alg.2		Alg.3		Alg.3, C1+=2dB	
C1,C2	Missed	False	Missed	False	Missed	False	Missed	False
6.0dB	17.8%	10.91%	17.8%	4.06%	17.8%	3.48%	10.3%	4.15%
8.0dB	10.5%	6.57%	10.5%	2.42%	10.4%	1.71%	6.1%	1.92%
9.0dB	8.5%	5.09%	8.5%	1.81%	8.3%	1.16%	5.4%	1.28%
10.0dB	7.3%	4.01%	7.3%	1.42%	7.5%	0.79%	5.4%	0.85%
11.0dB	8.9%	3.14%	8.9%	1.06%	8.3%	0.51%	6.5%	0.54%
12.0dB	11.6%	2.53%	11.6%	0.85%	11.3%	0.33%	9.9%	0.35%
13.0dB	17.0%	2.07%	17.0%	0.67%	16.3%	0.22%	15.3%	0.23%
14.0dB	23.5%	1.70%	23.5%	0.54%	22.4%	0.14%	21.6%	0.15%
16.0dB	39.2%	1.21%	39.2%	0.35%	39.6%	0.06%	38.9%	0.06%
20.0dB	67.3%	0.65%	67.3%	0.14%	72.5%	0.01%	72.4%	0.01%

It is important to minimize both types of errors. If too much interference is missed, then the filter is not doing an adequate job of cleaning up the received signal. If the false alarm rate is too high, then background damage is done at all times and the overall signal quality (especially sub-clutter visibility) may be compromised. We suggest that you try to keep the false alarm rate fairly low, perhaps below 1%; and then let the missed percentage fall where it may.

To summarize the numerical results in Table 5–2:

- The "Missed" rates of Alg.1 and Alg.2 are identical, but the "False" rate of Alg.1 is much higher. Alg.1 clearly does not perform as well for additive interference, but it is included in the suite for historical reasons.
- The "Missed" error rate for Alg.3 is nearly identical to that of Alg.2, but Alg.3 has a significantly lower false alarm rate. This is because of the somewhat improved statistics that result when the linear mean of P_{n-2} and P_{n-1} is used in the second comparison, rather than just P_{n-1} by itself. We recommend that Alg.3 generally be chosen in preference to the other two.
- Alg.3 can be further tuned by allowing the two constants to differ. For example, by raising C_1 slightly above C_2 (fourth column), we can trade off a decrease in the "Missed" rate for an increase in the "False" rate. Lowering C_1 would have the opposite effect.

Keep in mind that optimum tuning will depend on the type of interference you are trying to remove. In the previous example, where the interfering signal is only 16dB stronger than the weather, there was a close tradeoff between the "Missed" and "False" error rates. However, Table 5–3 shows the results that would be obtained if the interference dominates by 26db.

Table 5–3: Algorithm Results for +26dB Interference

	Alg.1		Alg.2		Alg.3		Alg.3, C2+=5dB	
C1,C2	Missed	False	Missed	False	Missed	False	Missed	False
6.0dB	17.8%	10.75%	17.8%	3.95%	17.8%	3.44%	17.8%	0.34%
8.0dB	9.9%	6.48%	9.9%	2.31%	9.9%	1.68%	9.9%	0.15%
9.0dB	7.4%	4.99%	7.4%	1.75%	7.4%	1.14%	7.4%	0.10%
10.0dB	5.9%	3.91%	5.9%	1.36%	5.9%	0.76%	5.9%	0.06%
11.0dB	4.8%	3.06%	4.8%	1.06%	4.8%	0.50%	4.8%	0.04%
12.0dB	3.2%	2.37%	3.2%	0.83%	3.2%	0.33%	3.2%	0.03%
13.0dB	2.6%	1.83%	2.6%	0.62%	2.6%	0.20%	2.8%	0.01%
14.0dB	1.9%	1.45%	1.9%	0.50%	1.9%	0.12%	2.6%	0.01%
16.0dB	1.3%	0.90%	1.3%	0.30%	1.3%	0.05%	5.8%	0.00%
20.0dB	3.1%	0.39%	3.1%	0.12%	2.0%	0.01%	31.5%	0.00%

Notice that we can now re-tune the constants and operate with $C_1 = 13dB$ and $C_2 = 18dB$ (fourth column); which yields a low 2.8% "Missed" rate, and an extremely low 0.01% false alarm rate. Since the false alarm rate is (approximately) independent of the interference power, these filter settings would leave all "clean" weather virtually untouched, i.e., we would have a very safe filter that is intended only to remove fairly strong interference. Such a filter could be left running at all times without too much worry about side effects.

5.1.6 Large-Signal Linearization

The RVP8 is able to recover the signal power of targets that saturate the IF-Input A/D converter by as much as 4–6 deciBels. This is possible because an overdriven IF waveform still spends some of its time in the valid range of the converter, and thus, it is still possible to deduce information about the signal.

Figure 5–2 shows actual signal generator test measurements with normal A/D saturation (lower line), and with the extrapolation algorithms turned on (upper line). The high-end linear range begins to roll off at approximately +10dBm versus +5dBm, and thus has been extended by 5dB.

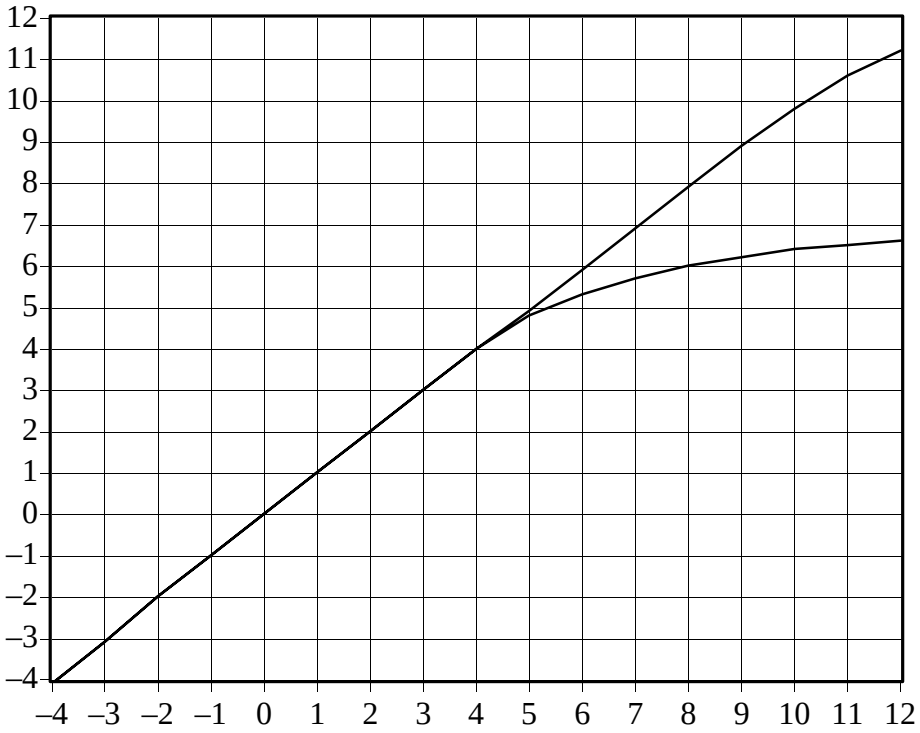

Figure 5–2: Linearization of Saturated Signals Above +4.5dBm (Rev B/C IFD)

The roll off starts at +4.5 dBm for the Rev. B&C IFD, and at +6 dBm for the Rev. D.

5.1.7 Correction for Tx Power Fluctuations

The RVP8 can perform pulse-to-pulse amplitude correction of the digital (I,Q) data stream based on the amplitude of the Burst/COHO input. The technique computes a (real valued) correction factor at each pulse by dividing the mean amplitude of the burst by the instantaneous amplitude of the burst. The (I,Q) data for that pulse are then multiplied by this scale factor to obtain corrected time series. The amplitude correction is applied after the Linearized Saturation Headroom correction.

The mean burst amplitude is computed by an exponential average whose *(1/e)* time constant is selected as a number of pulses (See Section 3.2.2). A short time constant will settle faster, but will not be as thorough in removing amplitude variations (since the mean itself will be varying).

Longer time constants do a better job, but will require a second or two before valid data is available when the transmitter is first turned on. The default value of 70 will give excellent results in almost all cases.

Whenever the RVP8 enters a new internal processing mode (time series, FFT, PPP, etc.), the burst power estimator is reinitialized from the level of the first pulse encountered, and an additional pipeline delay is introduced to allow the estimator to completely settle. Thus, valid corrected data are produced even when the RVP8 is alternating rapidly between different data acquisition tasks, e.g., in a multi-function ASCOPE display. The additional pipeline delay will not affect the high-speed performance when the RVP8 runs continuously in any single mode.

For amplitude correction to be applied, the instantaneous Burst/COHO signal level must exceed the minimum valid burst power specified in the "**Mb**" setup section. If that level is not met, e.g., if the transmitter is turned off, then no correction is performed. Thus, the amplitude correction feature conveniently "gets out of the way" when receiver-only tests are being performed.

The maximum correction that will ever be applied is $\pm$5dB. If the burst power in a given pulse is more than 5dB above the mean, or less than 5dB below it, then the correction is clamped at those limits. The power variation of a typical transmitter will easily be contained within this interval (it is typically less than 0.3dB).

Instantaneous amplitude correction is a unique feature of the RVP8 digital receiver. Bench tests with a signal generator reveal that an amplitude modulated waveform having 2.0dB of pulse-to-pulse variation is reduced to less than 0.02dB RMS of (I,Q) variation after applying the amplitude correction.

5.2 Time Series ("I" and "Q") Signal Processing

5.2.1 Time Series Processing Overview

This section describes the processing of the radar time series data (also called linear "video" or "I" and "Q") to obtain the meteorologically significant "moment" parameters: reflectivity, total power, velocity, width, signal quality index, clutter power correction, and optional polarization variables.

Recall that the time series synthesized by the FIR filter consist of an array of complex numbers:

$$s_m = [I_m + jQ_m] \quad \text{for} \quad m = 1, 2, 3, ..., M$$

where "j" is $-1^{1/2}$. The time series, are the starting point for all calculations performed within the RVP8. There are several excellent references on the details of I and Q processing. The reader is referred to Doviak and Zrnic's text on the subject. The top part of Figure 5–3 shows I and Q values for a simulated time series using the ascope utility.

There are two broad categories of time series signal processing:

- Time Domain Processing using the I and Q samples directly to calculate "autocorrelations" and then using the autocorrelations to compute the moments. This is used by many systems since the algorithms are very efficient requiring minimal storage and computational power. However, time domain algorithms are generally not adaptive or very flexible.
- Frequency Domain Processing using the I and Q samples to calculate a Doppler power spectrum and then applying algorithms, such as clutter filtering or 2nd trip echo filtering/extraction, in the frequency domain. The Doppler spectrum is then inverted to obtain the autocorrelation functions and these are used to calculate the moments. The frequency domain is well suited to more complex adaptive algorithms, i.e., where the processing algorithm is optimized for the data.

The RVP8 supports the concept of "major modes" or processing modes to process the time series. Currently the following major modes are supported by SIGMET:

- DFT/FFT Mode is a frequency domain approach which is used for most operational processing applications. There are a variety of clutter filtering options, including the GMAP algorithms (Gaussian Model Adaptive Processing).
- Pulse Pair Processing or PPP Mode is a time domain approach that is used primarily for dual polarization applications.
- Random Phase Mode or RPHASE is a frequency domain approach similar to the DFT/FFT, except that filtering and extraction of both the first and second trip echoes is supported.
- Batch Mode during which a small batch of low PRF pulses is transmitted (e.g., for 0.1 degree of scanning) followed by a large batch of higher PRF pulses (e.g., for 0.9 degrees of scanning) to determine which ranges are likely contaminated by second trip echo. This

was developed to support a US WSR88D legacy requirement. It is not supported in SIGMET's IRIS software.

The time and frequency domain approaches are described in the sections below.

Figure 5–3: Example of time series and Doppler power spectrum

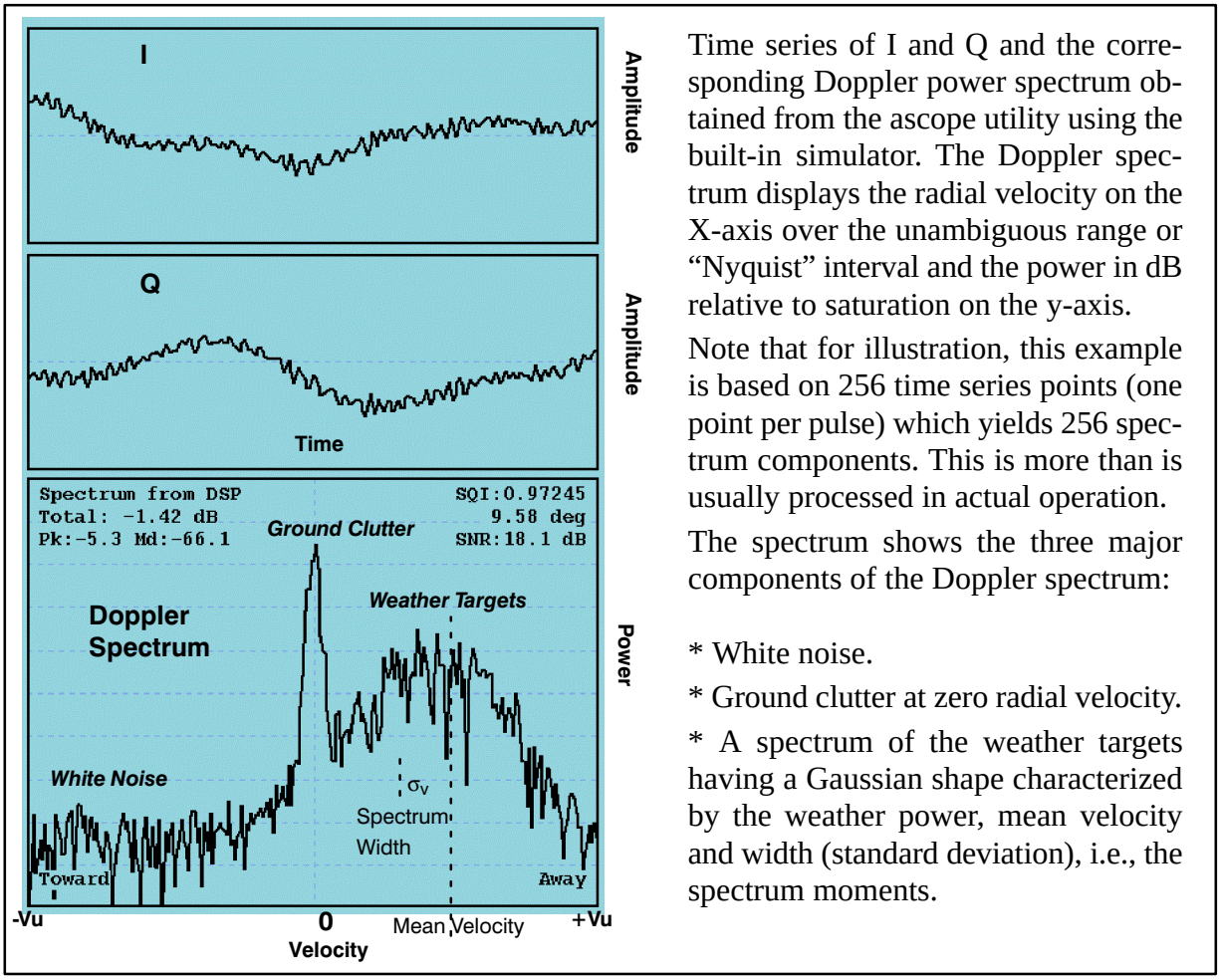

Time series of I and Q and the corresponding Doppler power spectrum obtained from the ascope utility using the built-in simulator. The Doppler spectrum displays the radial velocity on the X-axis over the unambiguous range or "Nyquist" interval and the power in dB relative to saturation on the y-axis.

Note that for illustration, this example is based on 256 time series points (one point per pulse) which yields 256 spectrum components. This is more than is usually processed in actual operation.

The spectrum shows the three major components of the Doppler spectrum:

* White noise.
* Ground clutter at zero radial velocity.
* A spectrum of the weather targets having a Gaussian shape characterized by the weather power, mean velocity and width (standard deviation), i.e., the spectrum moments.

5.2.2 Frequency Domain Processing- Doppler Power Spectrum

The Doppler power spectrum, or simply the "Doppler spectrum", is the easiest way to visualize the meteorological information content of the time series. The bottom part of Figure 5–3 shows an example of a Doppler power spectrum for the time series shown in the upper part of the figure. The figure above shows the various components of the Doppler spectrum, i.e., typically there is white noise, weather signal and ground clutter. Other types of targets such as sea clutter, birds, insects, aircraft, surface traffic, second trip echo, etc. may also be present.

The "Doppler power spectrum" is obtained by taking the magnitude squared of the input time series, i.e. for a continuous time series,

$$S(\omega) \quad = \quad |\mathcal{F}\{s(t)\}|^2$$

Here S denotes the power spectrum as a function of frequency ω, and $\mathcal{F}$ denotes the Fourier transform of the continuous complex time series s(t). The Doppler power spectrum is real-valued since it is the magnitude squared of the complex Fourier transform of s(t).

In practice a pulsed radar operates with discrete rather than continuous time series, i.e., there is an I and Q value for each range bin for each pulse. In this case we use the discrete Fourier transform or DFT to calculate the discrete power spectrum. Note that in the special case when we have 2^n input time series samples (e.g., 16, 32, 64, 128, ...), we use the fast Fourier transform algorithm (FFT), so called because it is significantly faster than the full DFT.

The DFT has the form:

$$S_k \quad = \quad |DFT_k\{w_m s_m\}|^2 \quad = \quad \left| \sum_{m=0}^{M} w_m s_m e^{-j(2\pi/M)mk} \right|^2$$

Typically a weighting function or "window" w_m is applied to the input time series s_m to mitigate the effect of the DFT assumption of periodic time series. The RVP8 supports different windows such as the Hamming, Blackman, Von Han, Exact Blackman and of course the rectangular window for which all spectral components are weighted equally. The typical form of a spectrum

window is shown in the figure below which illustrates how the edge points of the time series are de–emphasized and the center points are over emphasized. The dashed line would correspond to the rectangular window. Note that the "gain" of the window is set to preserve the total power.

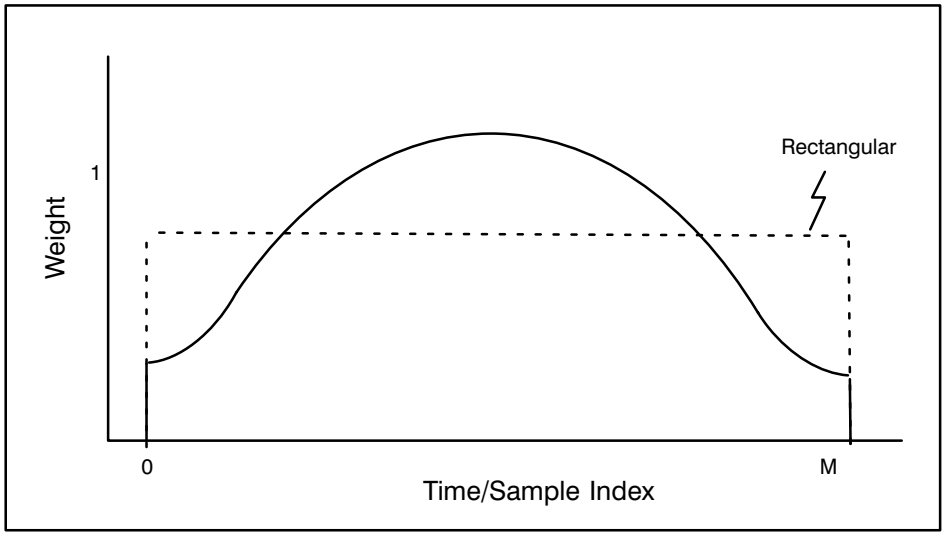

Figure 5–4: Typical form of a time series window

Even though the window gain can be adjusted to conserve the total power, there is an effective reduction in the number of samples which increases the variance (or uncertainty) of the moment estimates. For example the variance of the total power is greater when computed from a spectrum with Blackman weighting as compared to using a rectangular window. This is because there are effectively fewer samples because of the de-emphasis of the end points. This is a negative side to using a window.

The DFT of the window itself is known as its impulse response which shows all of the frequencies that are generated by the window itself. A generic example is shown in Figure 5–5 below which illustrates that these "side lobe" frequencies can have substantial power. This is not a problem for weather signals alone, but if there is strong clutter mixed in, then the side lobe power from the clutter can obscure the weaker weather signals. The rectangular window has the worst sidelobes, but the narrowest window width. However, the rectangular window provides the

lowest variance estimates of the moment parameters (in the absence of clutter. More "aggressive" windows have lower side lobe power at the expense of a broader impulse response and an increased variance of the moment estimates.

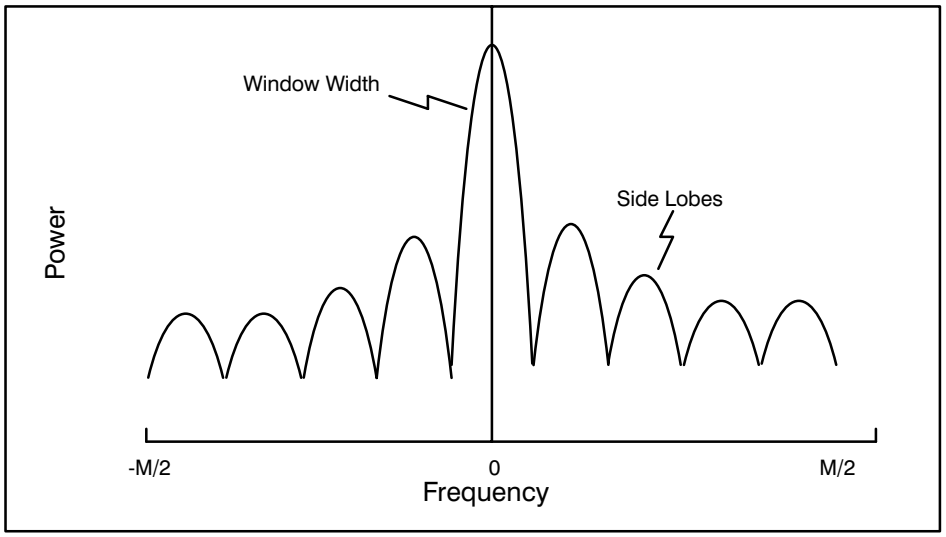

Figure 5–5: Impulse response of a typical window

So in summary of the DFT approach and spectrum windows:

- When the clutter is strong, an aggressive spectrum window is required to contain the clutter power so that the side lobes of the window do not mask the weather targets. The side lobe levels of some common windows are:

Rectangular	12 dB
Hamming	40 dB
Blackman	55 dB

- More aggressive windows typically have a wider impulse response. This effectively increases the spectrum width. Rectangular is narrow, Hamming intermediate and Blackman the widest.
- Windows effectively reduce the number of samples resulting in higher variance moment estimates. Rectangular is the best case, Hamming is intermediate and Blackman provides the highest variance moment estimates.

These facts suggest the best approach is to use the least aggressive window possible in order to contain the clutter power that is actually present- i.e., an adaptive approach is the best.

5.2.3 Autocorrelations

The final spectrum moment calculation (for total power or SNR, mean velocity and spectrum width) in all processing modes is based on autocorrelation moment estimation techniques. Typically the first three lags are calculated, denoted as R_0, R_1 and R_2. However, there are two ways to calculate these, i.e., time domain or frequency domain calculation. In the PPP mode for dual polarization, the autocorrelations are computed directly in the time domain while in the DFT mode, they are computed by taking the inverse DFT the Doppler power spectrum in the frequency domain. Note that only the first three terms need be calculated in the inverse DFT case. The time domain and frequency domain techniques are nearly identical except that the method of taking the inverse DFT of the power spectrum relies on the assumption that the time series is periodic. Another difference is that for time domain calculation only a rectangular weighting is used.

The time domain calculation of the autocorrelations and the corresponding physical models are:

Parameter and Definition	**Physical Model**
$T_o = \frac{1}{M}\sum_{n=1}^{M} s_n^* \; s_n$	$g^r g^t \; (S + C) + N$
$R_o = \frac{1}{M}\sum_{n=1}^{M} s'^*_n \; s'_n$	$g^r g^t \; S + N$
$R_1 = \frac{1}{M-1}\sum_{n=1}^{M-1} s'^*_n \; s'_{n+1}$	$g^r g^t \; S \; e^{\,j\,\pi\,V' \;-\; \pi^2\,W^2/2}$
$R_2 = \frac{1}{M-2}\sum_{n=1}^{M-2} s'^*_n \; s'_{n+2}$	$g^r g^t \; S \; e^{\,j\,2\pi\,V' \;-\; 2\pi^2\,W^2}$

where M is the number of pulses in the time average. Here, s' denotes the clutter-filtered time series, s denotes the original unfiltered time series and the * denotes a complex conjugate. g^r and g^t represent the transmitter and receiver gains, i.e., their product represents the total system gain. Since the RVP8 is a linear receiver, there is a single gain number that relates the measured autocorrelation magnitude to the absolute received power. However, since many of the algorithms do not require absolute calibration of the power, the gain terms will be ignored in the discussion of these. T_o for the unfiltered time series is proportional to the sum of the meteorological signal S, the clutter power C and the noise power N. R_0 is equal to the sum of the meteorological signal S and noise power N which is measured directly on the RVP8 by periodic noise sampling. T_o and R_0 are used for calculating the dBZ values- the equivalent radar reflectivity factor which is a calibrated measurement. The physical models for R_0, R_1 and R_2 correspond to a Gaussian weather signal and white noise as shown in Figure 5–3. W is the spectrum width and V' the mean velocity, both for the normalized Nyquist interval on [–1 to 1].

The autocorrelation lags above and the corresponding physical models have five unknowns: N, S, C, V', W. Because the R1 and R2 lags are complex, this yields, effectively, five equations in five unknowns using the constraint provided by the argument of R1. This closed system of equations can be solved for the unknowns which is the basis for calculating the moments from the autocorrelations.

5.2.4 Angle Synchronization

The exact value of *M* that is used for each time average will generally be the "Sample Size" that is selected by the SOPRM command (See Section 6.3). However, when the RVP8 is in PPP mode and antenna angle synchronization is enabled, the actual number of pulses used may be limited by the number that fit within each ray's angular limits at the current antenna scan rate. The value of *M* will never be greater than the SOPRM Sample Size, but it may sometimes be less. For example, at 1KHz PRF, 20°/sec scan rate, 1° ray synchronization, and a Sample Size of 80, there will be 50 pulses used for each ray (not 80). Note, however, that the number of pulses used in the "batched" (non-PPP) modes will always be exactly equal to the Sample Size, since those modes are allowed to use overlapping pulses.

5.2.5 Clutter Filtering Approaches

Each major mode implements clutter filtering as follows:

- DFT Mode uses frequency domain clutter filters.
- PPP Mode, used only for dual polarization. No clutter filtering is done in the PPP mode since this will typically damage the polarization information.
- Random Phase Mode uses frequency domain clutter filters.
- Batch Mode uses a simple DC removal for the small batch clutter filter. The high PRF large batch is then processed using the DFT mode.

In previous versions of SIGMET processors, an IIR (infinite implodes response) filter was offered. The IIR filter, while requiring minimal storage and computation, has three major drawbacks:

- The infinite impulse response requires a settling time when a transient occurs such as a PRF change, or a spike clutter target. During the settling time, the transient response degrades the performance of the filter.
- The filter is fixed width in the Nyquist interval. This means that it may be sufficiently wide to remove moderate or weak clutter, but may not be wide enough to remove all of the clutter when the clutter power is very strong and consequently wider in the Nyquist interval. This causes operators to select wider filters than necessary so that strongest clutter is adequately removed.
- The filter does significant damage to overlapped (zero velocity) weather signals, i.e., these will be significantly attenuated by the filter.

With the advent of the high speed processors such as the RVP8, there is sufficient storage and computational power to implement frequency domain filters that, in some cases, are adaptive. Because of the superiority of these filters, the legacy time domain IIR approach is no longer used in the RVP8. The only mode that uses time domain filtering is the Batch mode for the low PRF pulses (subtraction of the average I and Q to remove the DC component).

The various frequency domain filters available in the RVP8 are configured using the "mf" setup command (Section 3.2.3). These are:

- Type 0: Fixed width filters with interpolation
- Type 1:Variable width single slope adaptive processing
- Type 2: Gaussian model adaptive processing (GMAP)

These filters are described in in the sections detail below.

5.2.5.1 Fixed Width Clutter Filters

This filter, illustrated in Figure 5–6, removes a specified number of spectrum components (5 in the example) and then interpolates across the gap using the minimum of a specified number of "edge points" (2 in the example) to anchor the interpolation at each end of the gap. This is a fairly simple legacy approach that uses interpolation to repair the damage caused by the removal of components.

Figure 5–6: Example of fixed width

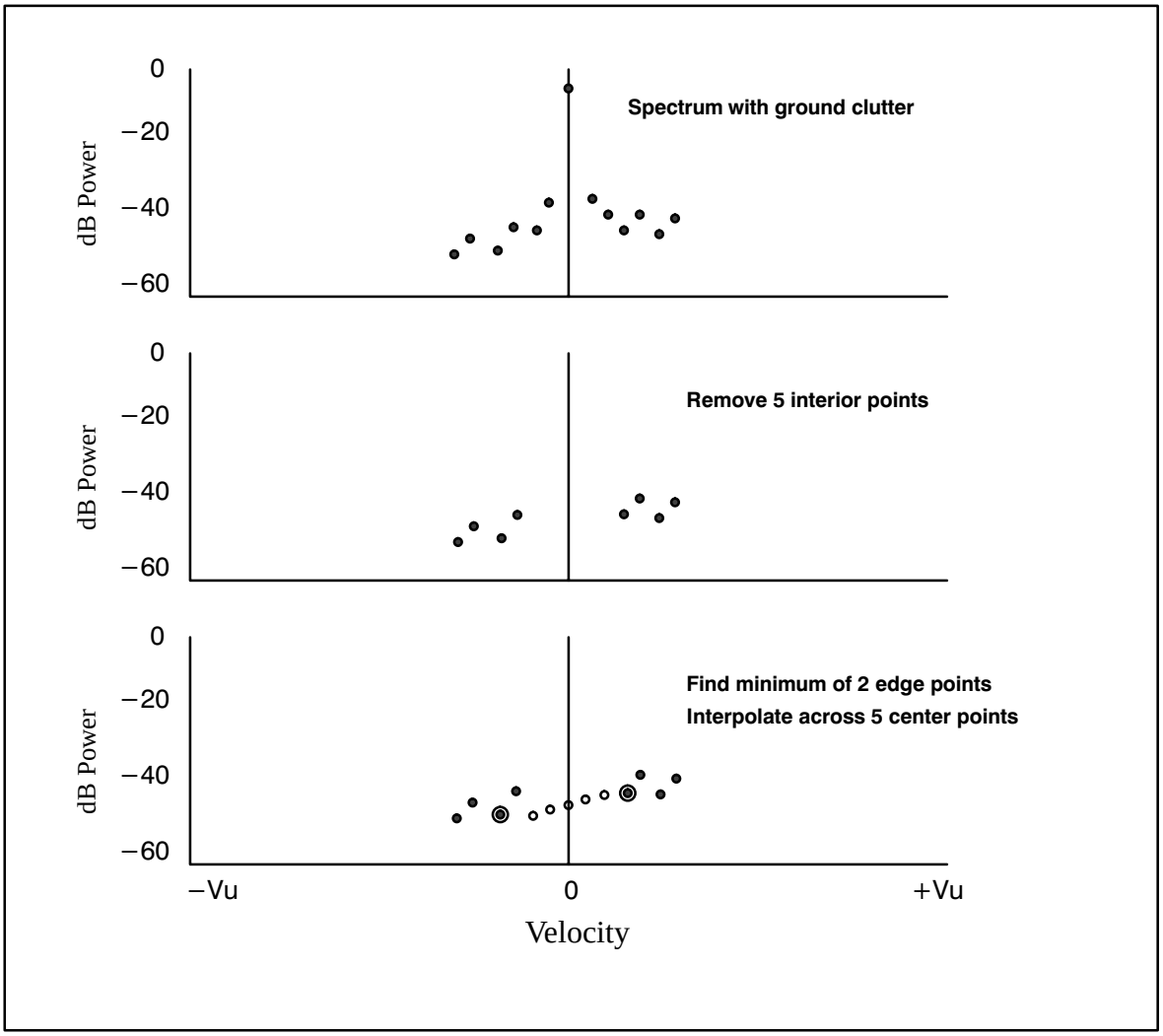

This procedure attempts to preserve the noise level and/or overlapped weather targets. The result is that more accurate estimates of dBZ are obtained. In extreme cases when the weather spectrum is very narrow, there can still be some attenuation of weather of a broad filter is selected.

5.2.5.2 Variable Width Clutter Filter

This is similar in many ways to the fixed width filter except that the algorithm attempts to extend the boundary of the clutter by determining which is the first component outside the clutter region to increase in power. The filter is illustrated in the figure below.

Figure 5–7: Variable Width Clutter Filter

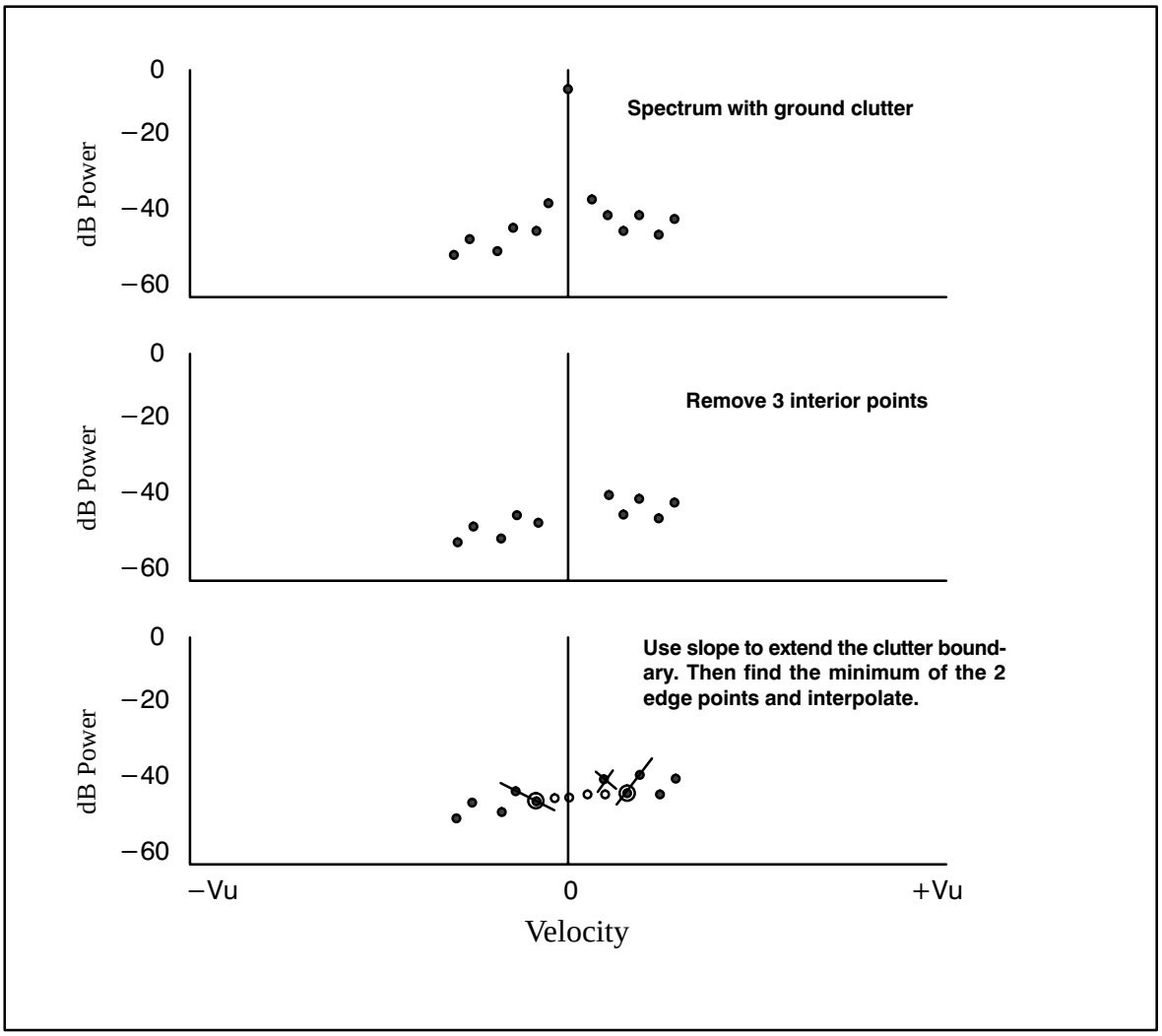

In the example above, the minimum number of points to reject is set to 3. The filter starts at zero velocity and checks the slope to determine the point at which the power starts to increase. In the example, this results in the filter being extended by one point on the right. Note that there is a selectable maximum number of points that the filter will "hunt". The use of the edge points for interpolation is identical to the fixed width case.

This filter allows users to specify a narrower nominal filter than the fixed width case and then when the clutter is strong, this width is extended by the algorithm (the "hunt"). The interpolation attempts to preserve any overlapped clutter and weather.

5.2.5.3 Gaussian Model Adaptive Processing (GMAP)

GMAP is a new adaptive technique developed at SIGMET that is possible on a high-speed processor such as the RVP8. GMAP has the following advantages as compared to fixed width frequency domain filters or time domain filtering such as the IIR approach:

- The width adapts in the frequency domain to adjust for the effects of PRF, number of samples and the absolute amplitude of the clutter power. This means that minimal operator intervention is required to set the filter.
- If there is no clutter present, then GMAP does little or no filtering.
- GMAP repairs the damage to overlapped (near zero velocity) weather targets.
- The DFT window is determined automatically to be the least aggressive possible to remove the clutter. This reduces the variance of the moment estimates.

The GMAP algorithm is described below.

GMAP Model Assumptions

GMAP makes several assumptions about the model for clutter, weather and noise, i.e.,

- The spectrum width of the weather signal is greater than that of the clutter. This is a fundamental assumption required of all Doppler clutter filters.
- The Doppler spectrum consists of ground clutter, a single weather target and noise. Bi-modal weather targets, aircraft or birds mixed with weather would violate this assumption.
- The width of the clutter is approximately known. This is determined primarily by the scan speed and to a lesser extent by the climatology of the local clutter targets. The assumed width is used to determine how many interior clutter points are removed.
- The shape of the clutter is approximately Gaussian. This shape is used to calculate how many interior clutter points are removed.
- The shape of the weather is approximately Gaussian. This shape is used to reconstruct filtered points in overlapped weather.

GMAP Algorithm Steps

The steps used to implement the GMAP approach are shown schematically in Figure 5–8 and summarized below.

- **Step 1: Window and DFT**
  First a Hamming window weighting function is applied to the IQ values and a discrete Fourier transform (DFT) is then performed. This provides better spectrum resolution than a fast Fourier Transform (FFT) which requires that the number of IQ values be a power of 2. Note that if the requested number of samples is exactly a power of 2, then an FFT is used.

Figure 5–8: GMAP Algorithm Steps

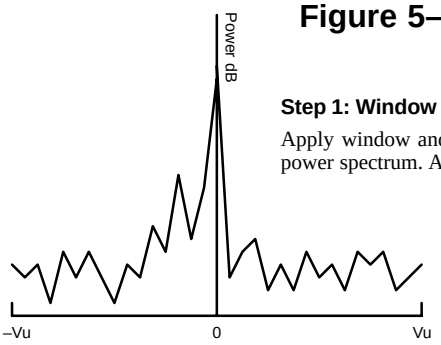

Step 1: Window and DFT

Apply window and DFT the input time series to obtain the Doppler power spectrum. A Hamming window is used for the first trial.

Step 2 (Optional): Dynamic noise power

If the noise level is not known, or if GMAP is recalculated using the Blackman window for CSR>40 dB, then this step is performed. Re-organize the spectrum components in ascending order of intensity. The theoretical relationship for noise is the curved line. The sum of the power in the range 5% to 40% is calculated. This is used to determine the noise level by comparing with the sum value corresponding to the theoretical curve. Next, the power is summed beyond the 40% point for both the actual and theoretical rank spectra. The point where the actual power sum exceeds the theoretical value by 2 dB determines the boundary between the noise region and the signal/clutter region.

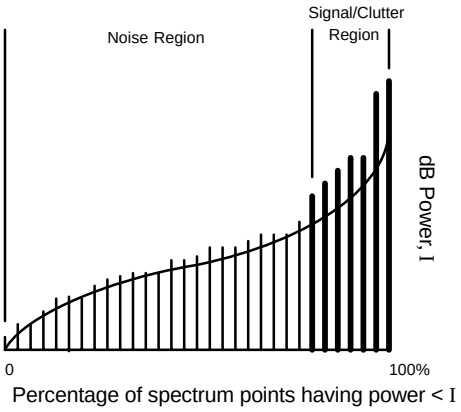

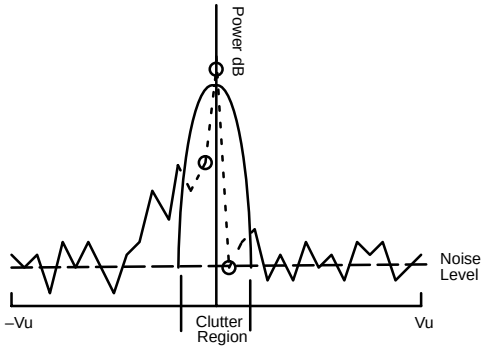

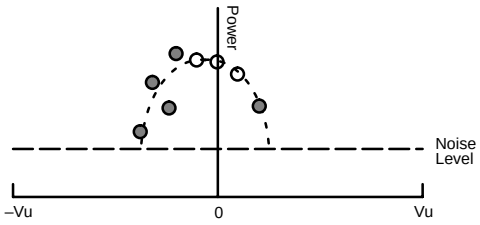

Step 3: Remove clutter points

Use the total power of the three central spectrum points (indicated by the three open circles) to fit a Gaussian having the selected nominal spectrum width in m/s (a function of the number of spectrum samples, PRF and wavelength). The points within the intersection of the Gaussian clutter and the noise level (the "Clutter Region") are discarded (indicated by the dashed lines).

Step 4: Replace clutter points

Dynamic Noise Case: Using the components which have been determined to be neither clutter nor noise (indicated by the filled circles), fit a Gaussian and fill-in the clutter points that were removed in the previous step (indicated by the open circles). Then re-fit the Gaussian with the replacement values inserted. Repeat the iteration until the computed power does not change by more than 0.2dB AND the velocity does not change by more than 0.5% of the Nyquist velocity.

Fixed Noise Case: Similar except the spectrum points that are larger than the noise level are used.

Step 5: Recompute GMAP with optimal window

Determine if the optimal window was used based on the clutter-to-signal ratio (CSR)

IF CSR > 40 dB repeat GMAP using a Blackman window and dynamic noise calculation.

IF CSR > 20 dB repeat GMAP using a Blackman window. Then if CSR>25dB use Blackman results.

IF CSR < 2.5 dB repeat GMAP using a rectangular window. Then if CSR < 1 dB use rectangular results.

ELSE accept the Hamming window result.

- As mentioned in Section 5.2.2, when there is no or very little clutter, use of a rectangular weighting function leads to the lowest-variance estimates of intensity, mean velocity and spectrum width. When there is a very large amount of clutter, then the aggressive Blackman window is required to reduce the "spill-over" of power from the clutter target into the sidelobes of the impulse response function. The Hamming window is used as the first guess. After the first pass GMAP analysis is complete, a decision is made to either accept the Hamming results, or recalculate for either rectangular or Blackman depending on the clutter-to-signal ratio (CSR) computed from the Hamming analysis. The recalculated results are then checked to determine whether to use these or the original Hamming result (see Figure 5–8 for details).

- **Step 2: Determine the noise power**
  In general, the spectrum noise power is known from periodic noise power measurements. Since the receiver is linear and requires no STC or AGC, the noise power is well–behaved at all ranges. The only time that the spectrum noise power will differ from the measured noise power is for very strong clutter targets. In this case, the clutter contributes power to all frequencies, essentially increasing the spectrum noise level. This occurs for two reasons: 1) In the presence of very strong clutter, even a small amount of phase noise causes the spectrum noise level to increase, and 2) There is significant power that occurs in the window side-lobes. For a Hamming window, the window side lobes are down by 40 dB from the peak at zero velocity. Thus 50 dB clutter targets will have spectrum noise that is dominated by the window sidelobes in the Hamming case. The more aggressive Blackman window has approximately 55 dB window sidelobes at the expense of having a wider impulse response and larger negative effect on the variance of the estimates.

- When the noise power is not known, it is optionally computed using a dynamic approach similar to that of Hildebrand and Sekhon (1974). The Doppler spectrum components are first sorted in order of their power. As shown in Figure 5–8, the sorting places the weakest component on the left and the strongest component on the right. The vertical axis is the power of the component. The horizontal axis is the percentage of components that have power less than the y-axis power value. Plotted on a dB scale, Poisson distributed noise has a distinct shape, as shown by the curved line in Figure 5–8. This shape shows a strong singularity at the left associated with taking the log of numbers near zero, and a strong maximum at the right where there is always a finite probability that a few components will have extremely large values.

- There are generally two regions: a noise region on the left (weaker power) and a signal/clutter region on the right (stronger power). The noise level and the transition between these two regions is determined by first summing the power in the range 5% to 40%. This sum is used to determine the noise level by comparing with the sum value corresponding to the theoretical curve. Next, the power is summed beyond the 40% point for both the actual and theoretical rank spectra. The point where the actual power sum exceeds the theoretical value by 2 dB determines the boundary between the noise region and the signal/clutter region.

- Finally there are two outputs from this step: a spectrum noise level and a list of components that are either signal or clutter
- **Step 3: Remove the clutter points**
  The inputs for this step are the Doppler power spectrum, the assumed clutter width in m/s and the noise level, either known from noise measurement or optionally calculated from the previous step. First the power in the three central spectrum components is summed (DC ±1 component) and compared to the power that would be in the three central components of a normalized Gaussian spectrum having the specified clutter width and discretized in the identical manner. This serves as a basis for normalizing the power in the Gaussian to the observed power. The Gaussian is extended down to the noise level and all spectral components that fall within the Gaussian curve are removed. The power in the components that are removed is the "clutter power".
- A subtle point is the use of the three central points to do the power normalization of the actual vs the idealized spectrum of clutter. This is more robust than using a single point since for some realizations of clutter targets viewed with a scanning antenna, the DC component is not necessarily the maximum. Averaging over the three central components is a more robust way to characterize the clutter power.
- The very substantial algorithmic work that has been done thus far is to eliminate the proper number of central points. The operator only has to specify a nominal clutter width in m/s. This means that the operator does not need to consider the PRF, wavelength or number of spectrum points- GMAP accounts for these automatically.
- A key point is that in the event that the sum of the three central components is less than the corresponding noise power, then it is assumed that there is no clutter and all of the moments are then calculated using a rectangular window. If the power in the three central components is only slightly larger than the noise level, then the computed width for clutter removal will be so narrow that only the central (DC) point shall be removed. This is very important since, if there is no clutter then we want to do nothing or at worst only remove the central component.
- Because of this behaviour, there is no need to do a clutter bypass map, i.e., turn-off the clutter filter at specific ranges, azimuths and elevation for which the map declares that there is no clutter. Because of the day-to-day variations in the clutter and the presence of AP, the clutter map will often be incorrect. Since GMAP determines the no-filter case automatically and then processes accordingly, a clutter map is not required.
- **Step 4: Replace clutter points**
  The assumption of a Gaussian weather spectrum now comes into play to replace the points that have been removed by the clutter filter. There are two cases depending on how the noise level is determined under Step 2, i.e., the dynamic noise case and the fixed noise level case.
- **Dynamic noise level case:** From Step 2, we know which spectrum components are noise. From Step 3 we know which spectrum components are clutter. Presumably, everything that is left is weather signal. An inverse DFT using only these components is

performed to obtain the autocorrelation at lags 0, 1. This is very computationally efficient since there are typically few remaining points and only the first two lags need be calculated. The pulse pair mean velocity and spectrum width are calculated using the Gaussian model (e.g., see Doviak and Zrnic, 1993). Note that since the noise has already been removed, there is no need to do a noise correction. The Gaussian model is then applied using the calculated moments to determine a substitution value for each of the spectrum components that were removed in Step 3.

- In the case of overlapped weather as shown in the Figure 5–8 example, the replacement power is typically too small. For this reason, the algorithm recomputes R0 and R1 using both the observed and the replacement points and computes new replacement points. This procedure is done iteratively until the power difference between two successive iterations is less than 0.2 dB and the velocity difference is less than 0.5% of the Nyquist interval.
- In summary of this step, the Gaussian weather model is used to repair the filter bias, i.e., the damage that is caused by removing the clutter points. An IIR filtering approach makes no attempt to repair filter bias, rather the filter simply "digs a hole" into overlapped weather.
- **Step 5: Check for appropriate window and recalculate the moments if necessary.** The clutter power is known from the spectrum components that were removed in Step 3. Since the weather spectrum moments and the noise are also known from Step 4, the CSR can be calculated. The value of the CSR, is used to decide whether the Hamming window is the most appropriate. The scenarios are described in Figure 5–8. The end result is that very weak clutter is processed using a rectangular window, moderate clutter a Hamming window, while severe clutter requires a Blackman window. Note that if no clutter were removed in Step 3, then the spectrum is processed with a rectangular window.
- The benefit of adaptive windowing is that the least aggressive window is used for the calculation of the spectrum moments, resulting in the minimum variance of the moment estimates.

GMAP Configuration

The 'mf' command in the dspx TTY setups is used to configure GMAP filters. In the section for the spectrum filters select filter "Type 2" and specify the width of the ground clutter in m/s. This width is determined largely by your antenna rotation rate so you will want to configure several widths to deal with the different rotation rates in your operational scenario. An example might be filters indexed 1-5 corresponding to widths from 0.1 to 0.5.

A good practice is to make a scan on a clear day while using ascope or other utility and observe what the actual width of the clutter is for your various scan rates. You will need to turn-off the clutter filtering to do this (pick "filter 0" for the all pass filter).

Example of Implementation

GMAP has undergone extensive evaluation for use in the US WSR88D ORDA network upgrade (Ice et al, 2004). They conclude that GMAP meets the ORDA requirements. Their

study was based on a built-in simulator that is provided as part of the RVP8 and the ascope utility. The simulator allows users to construct Doppler spectra, process them and evaluate the results (Sirmans and Bumgarner, 1975). This is an essential tool for evaluating the system performance.

Figure 5–9 shows an example of the simulations for the very difficult case when the weather has zero velocity, i.e., it is perfectly overlapped with clutter. The upper left graph shows the weather signal with –40 dB power without any clutter and without any GMAP filtering. The graph at the upper right shows the same spectrum with 0 dB of clutter power added for a clutter width of 0.012 (0.3 m/s at S band, 1000 Hz PRF). This is a CSR of 40 dB. The panel at the lower left shows the weather signal after GMAP filtering.

In each of the moment plots, there are several values that are displayed. The left-most number shows the value at the range cursor which is positioned as indicated by the vertical line. To the right, the "m" value is the mean and the "s" value the standard deviation as averaged over all range bins (1000 in this example). For velocity these are in normalized units expressed as a fraction of the Nyquist interval. For reflectivity the values are in dB.

Some key points are:

- The mean velocity is correctly recovered as expected (the "m" value in the plot), but the standard deviation is higher (0.06 vs 0.04 in normalized units).
- The "Cor dBZ" shows 40.2 dB of "C.Rej". This is the difference between the "Tot dBZ" and the "Cor dBZ" values. The expected value is 40 dB in this case. This indicates that GMAP has recovered the weather signal in spite of the aggressive clutter filtering that is required.
- The standard deviation of the "Tot dBZ" is greater in the weather plus clutter (4.35 normalized units) as compared to the weather-only case. This is caused by the fluctuations in the clutter power in the Gaussian clutter model.
- The standard deviation of the Cor dBZ after GMAP filtering, while not as low as for the weather-only case are lower than the weather plus clutter case. In other words, the GMAP processing removes some of the high variance in the dBZ estimates that is caused by clutter, but is not quite as good as doing nothing.

Figure 5–9: GMAP example

Weather only

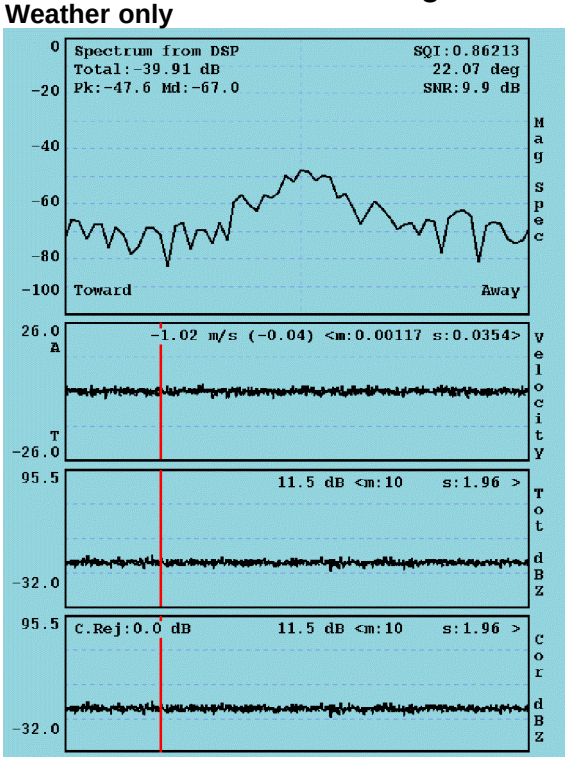

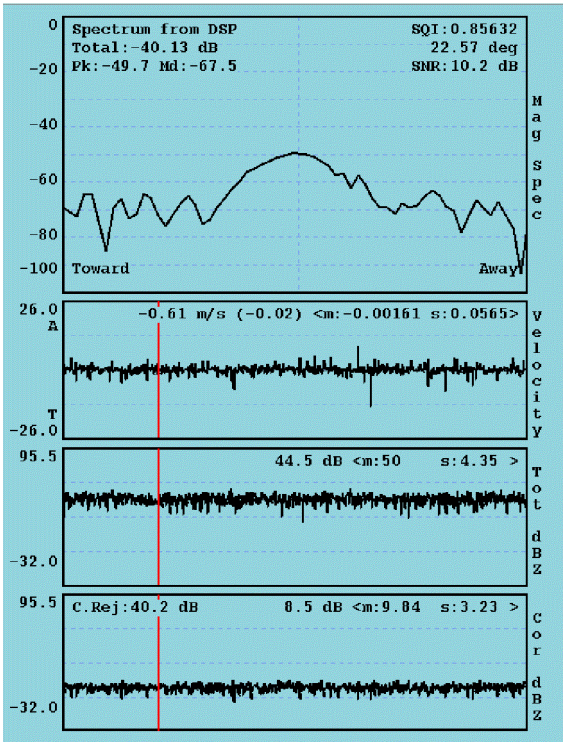

Weather plus clutter

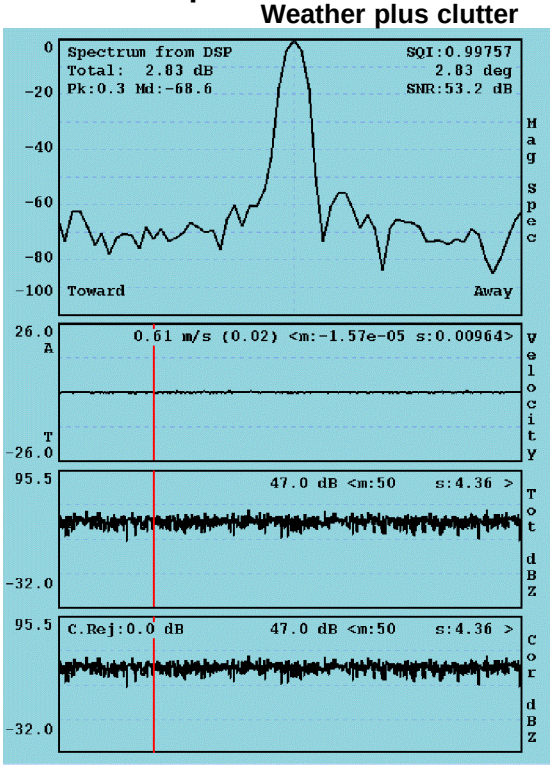

Simulation Characteristics

	Clutter	Weather	Units
Power	0	–40	dB
Vel	0	0	Any
Width	0.012	0.1	Normalized

PRF	1000 Hz	**Window**	Blackman
Mode	FFT	**Samples**	64

"Mag Spec": Doppler Spectrum in dB Units spanning the Nyquist interval.

"Velocity": Mean velocity of the spectrum in over Nyquist interval. Mean "m" and standard deviation values "s" are for the normalized interval ±1.

"Tot dBZ": Power in dB of weather and clutter. Mean "m" and standard deviation values "s" are in dB.

"Cor dBZ": Power in dB after GMAP filtering. Mean "m" and standard deviation values "s" are in dB.

"<m: ...s: ...>" mean and standard deviation over all ranges, in this case 1000 range bins.

5.2.6 Range averaging and Clutter Microsuppression

The next step (optional) is to perform range averaging. Range averaging can be performed over 2, 3, ..., 16 bins. This is accomplished by simply averaging the T_0, R_0, R_1 and R_2 values. This reduces the number of bins in the final output to save processing both in the RVP8 and in the host computer.

At the user's option, the range averaged data can be restricted to include only those bins which have an estimated clutter-to-signal ratio that falls within the CCOR threshold interval. By excluding isolated point clutter targets from the range average the sub-clutter visibility of the averaged data is increased. Specifically, the Doppler test that is applied to each bin in order that it contribute to the overall sum is:

$$10 \log R_0 - 10 \log T_0 > CCOR_{thresh} \ .$$

5.2.7 Reflectivity

The corrected reflectivity Z is output using a log scale based on the following equation:

$$dBZ = 10 \log\left[\frac{T_0 - N}{N}\right] + dBZ_o + 20 \log r + ar + CCOR$$

This equation is simply a dB version of the familiar radar equation for distributed targets. The relationship between the measured autocorrelation function, the received signal and the noise can be expressed as:

$$T_o = g^t g^r S + N$$

where g^t and g^r represent the transmitter and receiver gains, S is the average back scattered power from the targets and N is the measured average noise power. Neglecting attenuation and the contribution of ground clutter (for the moment), the radar equation can be written as.

$$Z = CSr^2 = \left[\frac{Cr_0^2 N}{g^r g^t}\right]\left[\frac{r^2}{r_o^2}\right]\left[\frac{T_o - N}{N}\right]$$

where C is the radar constant and r_o is a reference range which we will later set to 1 km. This is identical to the first three terms of the dB version of the equation with the definition that:

$$Z_o = \frac{Cr_o^2 N}{g^r g^t} = Cr_o^2 I_o \quad where \quad I_o = \frac{N}{g^r g^t}$$

Z_o is called the calibration reflectivity factor. It is the equivalent radar reflectivity factor at the reference range when the return signal power is equal to the noise power (SNR=0 dB). It is sometimes called the minimum detectable dBZ at 1 km, though it is more correct to call it the 0dB SNR detection level (See Figure 5–10). The parameter I_o is the measured noise power at IF with appropriate calibration for the system gain. Calibration of the RVP8 involves defining the radar constant C and measuring the value of I_o. This is discussed in detail in Section 5.4.

Essentially, the measurement of I_o is based on the measurement of the system noise at the time of calibration. However, if the receiver gain were to change after calibration, the use of periodic noise sampling properly corrects for this. For example, if the receiver gain were to change by a factor k, then we would measure a noise value of kN and an autocorrelation value of kT_o, i.e.,

$$Z = CSr^2 = \left[\frac{Cr_0^2 N}{g^r g^t}\right]\left[\frac{r^2}{r_o^2}\right]\left[\frac{k\ T_o - k\ N}{k\ N}\right]$$

Thus the k's cancel to give us the same result for Z. This makes the approach robust to system gain fluctuations. Another way of saying this is that as long as the system sensitivity (noise figure) does not change, then the system does not require re-calibration.

The individual terms in the dB form of the equation are summarized below.

1st Term : $10\log\left[\frac{T_0 - N}{N}\right]$: Signal to Noise Ratio

The effect of this term is to subtract the measured noise. It is also used for LOG thresholding. If this number is above the user input value LOG_{thresh} the dBZ is passed.

2rd Term: dBZ_o : Calibration Reflectivity (see discussion above)

dBZ_o is the minimum detectable dBZ at a reference range r_o=1 km,

3th Term: $20\log r$: Range Normalization

This term is the $\left[\frac{r}{r_o}\right]^2$ range normalization expressed in dB form.

4th Term: ar : Gaseous Attenuation Correction

This term accounts for gaseous attenuation. The constant a is set in the RVP8 EEROM since it is a function of wavelength. For a C-band system the default value is 0.016 dB per km (for two-way path attenuation).

5th Term: CCOR: Clutter Correction

This term corrects for the measured ground clutter. It's derivation is discussed in section 5.2.11.

5.2.8 Velocity

For a Doppler power spectrum that is symmetric about its mean velocity, the velocity is obtained directly from the argument of the autocorrelation at the first lag, i.e.,

$$V = \frac{\lambda}{4\pi\tau_s}\,\theta_1 \quad \text{where} \quad \theta_1 = \arg\{R_1\}.$$

λ is the radar wavelength, τ_s is the sampling time (1/PRF). θ_1 is constrained to be on the interval $[-\pi, \pi]$. When $\theta_1 = \pm\,\pi$, then $V = \pm\,V_u$ where the unambiguous velocity is ,

$$V_u = \frac{\lambda}{4\tau_s}.$$

If the absolute value of the true velocity of the scatterers is greater than V_u , then the velocity calculated by the RVP8 is folded into the interval $[-V_u\ ,\ V_u]$, which is called the Nyquist interval. Folding is usually easily recognized on a color display by a discontinuous jump in velocities. For example, if the true velocity is $V_u + \Delta V$, then the velocity calculated by the RVP8 is $-V_u + \Delta V$, which is $2V_u$ away from the true mean velocity.

For 8-bit outputs, rather than calculating the absolute velocity in scientific units, the RVP8 calculates the mean velocity for the normalized Nyquist interval [–1,1], i.e., the output values are,

$$V' = \frac{\theta_1}{\pi}.$$

For example, an output value of –0.5 corresponds to a mean velocity of $-V_u/2$. The normalized velocity V' is more efficient use of the limited number of bits.

5.2.9 Spectrum Width Algorithms

The spectrum width is a measure of the combined effects of shear and turbulence. To a lesser extent, the antenna rotation rate can also effect the spectrum width. At high elevation angles, the fall speed dispersion of the scatterers also effects spectrum width.

There are two choices for the spectrum width algorithm used in the RVP8, depending on the speed and accuracy that are required for the application:

R_0, R_1 "fast" algorithm valid when SNR >> 10 dB

R_0, R_1, R_2 "accurate" algorithm for SNR >> 0 to 5 dB

The approach used is selected in the SOPRM command. The two approaches are described below:

R_0, R_1 Width Algorithm

Given samples of the Doppler autocorrelation function, numerous estimates of spectral variance can be computed (Passarelli & Siggia, 1983). The particular estimator used by the RVP8 employs the magnitudes of R_0 and R_1 and assumes that the Doppler spectrum is Gaussian (usually an acceptable assumption) and that the signal-to-noise ratio is large. Specifically we have (similar to Srivastava, et al 1979):

$$Variance = 2\,\ln\left[\frac{R_o}{|R_1|}\right] = -2\,\ln[SQI]$$

where "ln" represents the natural logarithm. This can be compared to the expression in the preceding section for SQI to illustrate that this expression for the variance is only valid when:

$$\frac{SNR}{SNR + 1} \approx 1$$

which occurs when the SNR is large.

This variance estimator is normalized to the Nyquist interval in units of $[-\pi, \pi]$. Thus, for example, a variance of $\pi^2/25$ would be obtained from a Gaussian spectrum having a standard deviation equal to one fifth of the total width of the plotted spectral distribution. For scientific purposes, the spectrum width (standard deviation) is more physically meaningful than the variance, since it scales linearly with the severity of wind shear and turbulence. For these reasons, the width W is output by the RVP8:

$$W = \frac{\sqrt{Variance}}{\pi}$$

Again, for efficient packing in 8-bits, width is normalized to the Nyquist interval [–1, 1]. For the example given above, the output width W would be (1/5). To obtain the width in meters per second, one multiplies the output width by V_u .

R_0, R_1, R_2 Width Algorithm

The width algorithm in this case is similar except that the addition of R_2 extends the validity of the width estimates to weak signals. In this case the variance is:

$$Variance = \frac{2}{3} \ln\left[\frac{|R_1|}{|R_2|}\right]$$

The output width W is then defined as in the previous section.

5.2.10 Signal Quality Index (SQI threshold)

An important feature of the RVP8 is its ability to eliminate signals which are either too weak to be useful, or which have widths too large to justify further analysis. This is done via the signal quality index (SQI) which is defined as:

$$SQI = \frac{|R_1|}{R_0}$$

The SQI is the normalized magnitude of the autocorrelation at lag 1 and varies between 0 for an uncorrelated signal (white noise) to 1 for a noise-free zero-width signal (pure tone). Mean velocity estimates are degraded when the spectrum, width is large or when the signal-to-noise ratio is weak. The SQI is a good measure of the uncertainty in the velocity estimates and is a convenient screening parameter to compute. In terms of the Gaussian model, the SQI is :

$$SQI = \frac{SNR}{SNR + 1} e^{\frac{-\pi^2 W^2}{2}}$$

where the SNR is the signal-to-noise ratio. For very large SNR's the SQI is a function of the spectrum width only. For a zero-width pure tone (W=0), the SQI is a function of the SNR only (e.g., for W=0, an SNR of 1 corresponds to SQI=0.5). The SQI threshold is typically set to a value of 0.4 to 0.5.

5.2.11 Clutter Correction (CCOR threshold)

In addition to calculating the R_0, R_1 and optional R_2 autocorrelation terms, which are based on filtered time series data, the RVP8 also computes T_0 which is the total unfiltered power. By comparing the total filtered and unfiltered powers at each range bin, a clutter power, and hence a clutter correction, for that bin can be derived. The clutter correction is defined as,

$$CCOR = 10 \log \frac{S}{C+S} = 10 \log \frac{1}{CSR+1}$$

where S is the weather signal power, C is the clutter power and CSR is the clutter-to-signal ratio. The algorithm for calculating CCOR depends on whether the optional R_2 autocorrelation lag is computed as described below.

R_0, R_1 Clutter Correction

In this case CCOR is estimated from,

$$CCOR_{est} = 10 \log \left[\frac{R_0}{T_0} \right]$$

$$= 10 \log \left[\frac{S+N}{C+S+N} \right] = 10 \log \left[\frac{1 + \frac{1}{SNR}}{CSR + 1 + \frac{1}{SNR}} \right]$$

Here, the expression is strictly valid only when the signal-to-noise ratio (SNR=S/N) is large. Thus when the 2-lag approach is used, the clutter corrections are not as accurate for weak weather signals. However, the error is typically less than 3 dB.

R_0, R_1, R_2 Clutter Correction

In this case there is enough information to compute the clutter signal and noise power independently. The algorithm for CCOR is:

$$CCOR_{est} = 10 \log \frac{S}{C+S} = 10 \log \frac{1}{CSR+1}$$

The clutter power is computed from:

$$C = T_o - R_o = [C+S+N] - [S+N]$$

The signal power S is then computed from:

$$S = |R_1| \exp^{\frac{\pi^2 W^2}{2}}$$

W is the width that has been previously calculated. This approach yields more accurate results for the clutter correction in the case of a low SNR.

5.2.12 Weather Signal Power (SIG threshold)

A parameter called SIG is also calculated to provide an estimate of the weather signal-to-noise ratio in dB for thresholding. The SIG calculation is different depending on the whether the optional R_2 autocorrelation is computed.

R_0, R_1 Calculation

In this case the SIG is computed as follows:

$$SIG = 10 \log \left[\frac{T_0 - N}{N} \right] + CCOR$$

This term represents the SNR after the removal of clutter. The ***CCOR*** value is the one described for R_0, R_1 in the previous section.

R_0, R_1, R_2 Calculation

In this case the SIG is computed based on the SNR which is:

$$SIG = 10 \log \left[\frac{2\pi S}{R_0 - 2\pi S} \right]$$

where the signal power S is determined as described in the preceding section.

5.2.13 Signal to Noise Ratio (LOG threshold)

A parameter called LOG is also calculated to provide an estimate of the total signal-to-noise ratio in dB useful for reflectivity thresholding. The formula is below:

$$LOG = 10 \log \left[\frac{T_0 - N}{N} \right]$$

5.3 Thresholding

An important feature of the RVP8 is its ability to accept or reject incoming data based on derived properties of the signals themselves. Typically, "rejected" data are not displayed by the user's software, thus making for very clean weather presentations.

5.3.1 Threshold Qualifiers

For data quality control, each RVP8 output parameter can be qualified, i.e., either accepted or rejected for output, based on four threshold criteria:

ID	Criterion Name	Pass Criterion
LOG	Signal-to-Noise Ratio	LOG > threshold
SQI	Signal Quality Index	SQI > threshold
CCOR	Clutter Correction	CCOR > threshold
SIG	Weather Signal Power	SIG > threshold

The calculation of the measured levels (e.g., SQI) for each of these qualifications has been described in previous sections of this chapter. All four qualification criteria can be switched on and off independently, and the threshold levels (e.g., SQI_{thresh}) can each be set independently. Further, each qualifier test can be AND'd and OR'd with any other. This allows very complex thresholds criteria to be constructed as required. The four threshold qualifiers are summarized below.

LOG It is essentially a measure of the total power SNR. This is usually used for thresholding of the reflectivity data. The default LOG threshold value is 0.5 dB.

SQI The SQI threshold is typically used for velocity and width thresholding since it is a measure of the coherency. It is a number between 0 and 1 (dimensionless) where 0 is perfect white noise and 1 is a pure tone (perfect Doppler signal). The default SQI threshold value is 0.5.

CCOR The clutter correction threshold is typically used to reject measurements when the clutter in a range bin is very strong (i.e., when the calculated CCOR is a large negative number in dB). The appropriate value depends on the coherency of the radar system. The default threshold is set to –25 dB. Threshold values less than this (more negative) reject fewer clutter bins. Threshold values closer to zero reject more clutter bins.

SIG This is typically used only for thresholding the spectrum width to assure that the signal power is strong enough for an accurate width measurement. The default threshold value is 10 dB. If R_2 processing is used, this can usually be reduced to 5 dB for width thresholding.

The following are the default threshold combinations for each of the parameters that can be selected for output from the RVP8:

Parameter	Description	Threshold
dBZ	Reflectivity with clutter correction	LOG and CCOR
dBT	Reflectivity without clutter correction	LOG
V	Mean velocity	SQI and CCOR
W	Spectrum width	SQI and CCOR and SIG
ZDR	Differential reflectivity	LOG

5.3.2 Adjusting Threshold Qualifiers

The effect of the various threshold qualifiers for each output parameter are discussed in this section. In optimizing thresholds for your application, it is recommended that you change only one parameter (level or criterion) at a time so that you can verify the effect. Some hints for optimizing the levels for the default criteria are provided below:

LOG To optimize the LOG level, display dBT or dBZ and select the lowest value of the threshold that eliminates the display noise. If the LOG level is set too high you lose sensitivity. Note that if you average more pulses or ranges, then the threshold level can usually be reduced.

SQI To optimize the SQI level, display velocity and select the lowest value of the threshold that eliminates the display noise. If the SQI level is set too high you lose sensitivity. In general, you should see a greater area covered by velocity than reflectivity since the velocity is more sensitive. If you do not, you should reduce your SQI threshold. Note that if you average more pulses or ranges, then the threshold level can usually be reduced.

CCOR This is used to eliminate clutter targets that are very strong. It should not be set to eliminate all clutter targets on a clear day since this means that you are losing sensitivity. To optimize the CCOR threshold it is best to know your system coherency in terms of dB of clutter cancelation. Start at a value of 10 dB greater (closer to 0) than this. Now display a PPI of dBZ at an antenna elevation of ~1 degree. The display should be relatively clean of any clutter targets since most will be rejected. Now reduce the CCOR (more negative) to increase the number of clutter targets on the display until the number of clutter targets does not increase. The optimum value of the CCOR is approximately 5 dB more (closer to zero) than this point. For example, if the number of clutter targets is a maximum at –35 dB, then set the CCOR to ~–30 dB. Note that your clutter filter selection will effect the result.

SIG This should be done last. To optimize the SIG level, display the width W and select the lowest value of the threshold that eliminates the display noise. If the SIG level is set too high you lose sensitivity. Note that if you average more pulses or ranges, then the threshold level can usually be reduced.

When thresholding dBZ and dBT reflectivity data with SQI, the comparison value for accepting those data is the secondary SQI threshold that is defined via a slope and offset from the primary user value (see **Mf** command). This secondary threshold is more permissive (lower valued), and

is traditionally used to qualify LOG data only in the Random Phase processing mode. But the secondary SQI threshold is applied uniformly in all processing modes whenever reflectivity data are specified as being thresholded by SQI.

This gives you more freedom in applying an SQI threshold to your LOG data, because the cutoff value for reflectivity can be chosen independently from the cutoff value for the other Doppler parameters. The full SQI test would not normally be applied to LOG data because of the so-called "black hole" problem, i.e., loss of LOG data within regions of high shear, even though the reflectivity itself was strong. You may experiment with applying a secondary SQI threshold to help cleanup the LOG data, but without introducing any significant black holes.

5.3.3 Speckle Filters

A speckle filter is a final pass over each output ray, wherein isolated bins are removed. There are two speckle removers in the RVP8.

- 1D single-ray speckle filter. This can be used for any output parameter.
- 2D 3x3 speckle filter. If enabled, this is applied only to T, V, Z and W.

The 1D speckle filter is the default technique. The 2D 3x3 filter is enabled by selection in the mp TTY setups:

```
2D Final Speckle/Unfold "User" or "Always"
```

Both of these speckle filters remove isolated data points that are likely to be noise, interference, aircraft, birds or other point targets. Meteorological targets typically occupy multiple range bins so are not effected by the speckle filter. There are two primary benefits derived from using a speckle filter:

- Displays look "cleaner" to observers.
- Thresholds can be set slightly more sensitive without increasing the number of noise pixels.

The 2D 3x3 filter actually performs data filling of "missing speckles" as well as eliminating isolated speckle bins. The two algorithms are discussed below.

1D Speckle Filter

A ray is the basic azimuth unit of the RVP8 (e.g., 1 degree) over which the samples are averaged to obtain the output base data (T, Z, V, W). For this filter, a speckle is defined as any single, valid bin (not thresholded), having thresholded bins on either side of it in range. Any such isolated bin in a ray is set to "threshold". The algorithm is shown schematically below.

Note that there are two independent 1D speckle removers– one for the reflectivity data (dBT, dBZ and ZDR) and one for the Doppler data (V and W). Each one should be switched on or off, depending on the specific nature of the targets being observed. For example, when making a clutter map of the area, one would certainly want to switch both speckle filters off.

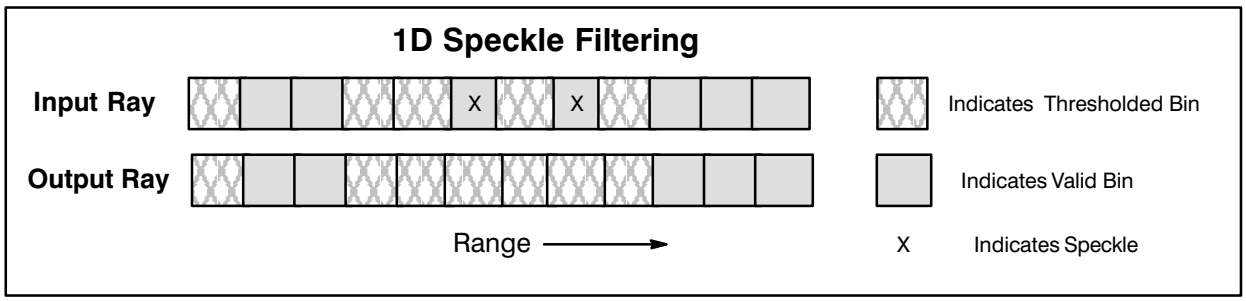

2D 3x3 Speckle Filter

The 2D filter examines three adjacent range bins from three successive rays in order to assign a value to the center point. Thus, for each output point, its eight neighboring bins in range and time are available to the filter. Only the dBZ, dBT, Vel , and Width data are candidates for this filtering step; all other parameters are processed using the default 1D speckle filter.

The rules for the filter are as follows:

	Center Point Action	
	Assign Threshold	**Else**
Valid Center Point	If there are no or only one other valid point in the 3x3.	Do Nothing. Pass the center point value as-is.
Thresholded Center Point	If there are 5 or fewer valid neighbors in the 3x3.	If there are 6 or more valid neighbors in the 3x3, average to fill the center point.

Thus the 2D 3x3 filter performs 2 functions:

- Filling by interpolation.
- Thresholding of isolated noise bins.

Some examples are shown graphically in the figure below.

For dBZ, dBT, and Width, the interpolated value for filling is computed as the arithmetic average of all available neighbors. For Vel , it is not possible to define a meaningful average in a simple way; so the nearest valid neighbor is simply filled in.

The filter has some interesting properties when combined with other algorithms.

Dual PRF Unfolding

Dual–PRF velocity unfolding is computed within the 3x3 filter whenever both are enabled. There are two steps to the process:

- Step 1: The most recent and the previous ray are used. For every valid point in the most recent ray, the algorithm performs a search among the three nearest neighbors in the previous ray to find a valid velocity. The search pattern is shown at the bottom of the previous figure. This larger selection of alternate–PRF bins makes it more likely that the algorithm will find the pairs of Low/High PRF data that are required for unfolding.

2D 3x3 Filtering Concepts

Threshold if center point is valid but there are no or only one valid neighbor.

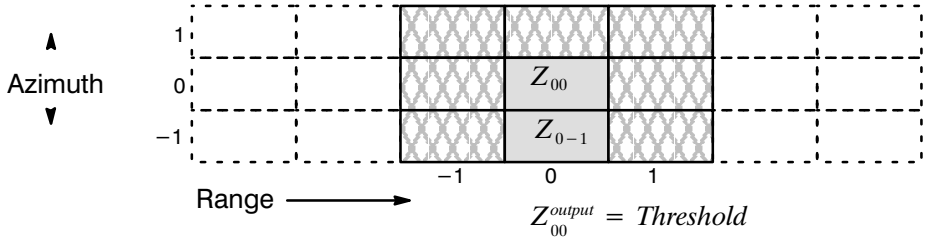

$$Z_{00}^{output} = Threshold$$

Fill thresholded center point with average if there 6 or more valid neighbors.

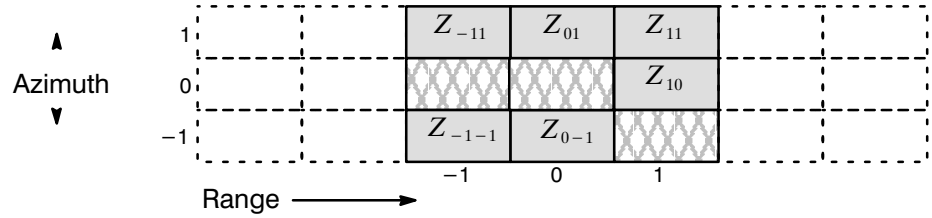

2D Velocity Unfolding Step 1: Search pattern for valid second velocity

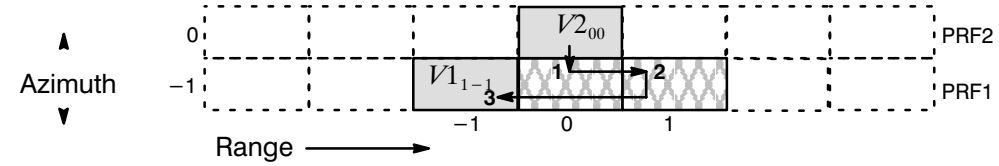


Indicates Thresholded Bin

$$Z_{00}^{output} = \frac{[Z_{-11} + Z_{01} + Z_{11} + Z_{10} + Z_{-1-1+}Z_{0-1}]}{6}$$

- Step 2: The unfolded velocities are then subjected to the standard 3x3 filtering.

Dual PRF, Random Phase Processing

In random phase processing, the "seam" at the start of the second trip is always problematic since the transmitter main bang and nearby clutter will virtually always wipe out the first few 2nd trip range bins. At a constant PRF the 2nd trip seam is always at the same range, but in dual PRF random phase mode, the seam is different each ray. Thus thresholded bins at the seam of the high PRF can be surrounded on either side by valid bins taken at the low PRF. The 3x3 filter has the effect of interpolating the reflectivity and width data over the bins at the 2nd trip seam. Velocity data will also be filled–in using the nearest neighbor. Thus the

2D filter mitigates much of the damage that is caused at the 2nd trip seam to make a nearly seamless display.

5.4 Reflectivity Calibration

The calculation of reflectivity described in Section 5.2.7 required the calibration reflectivity dBZ_o. This section describes it's derivation. Note that customers with the SIGMET IRIS system can use the **zauto** utility to perform the calibration. (See the *IRIS Utilities Manual.)*

Figure 5–10 Model Intensity Curve

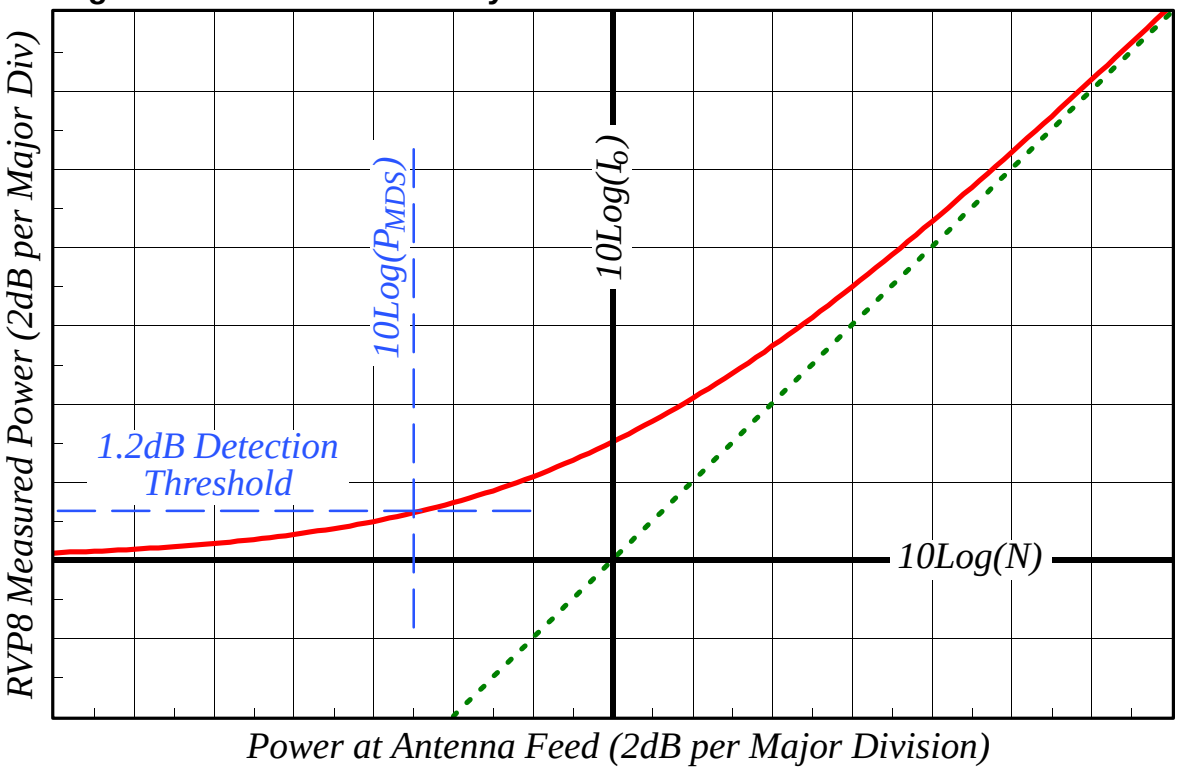

5.4.1 Plot Method for Calibration of I_o

This approach generates the curve shown above (red) which determines the value of I_o. The general procedure is to connect a calibrated signal generator to the radar receiver and inject known power levels to generate a calibration plot of measured power vs the inserted power at the antenna feed, similar to that in Figure 5–10. The calibration reflectivity dBZ_o is computed from the radar constant and the value of I_o, which is the intercept of the straight line fit (green) with the Noise level.

Why does this geometric construction yield the value of I_o ? Let G_{dB} represent the overall gain of the RF and IF components leading up to the RVP8. The green line can be interpreted as the response of an ideal noise-free amplifier having gain G_{dB}, while the red curve is the response of the real-world amplifier(s) whose equivalent front-end noise is I_o :

$$(Red) \quad 10\log_{10}(P_{OUT}) = G_{dB} + 10\log_{10}(P_{IN} + I_o)$$

$$(Green) \quad 10\log_{10}(P_{OUT}) = G_{dB} + 10\log_{10}(P_{IN})$$

The measured receiver noise is the horizontal asymptote of the red curve, i.e., the value of the red curve when the input power P_{IN} is zero:

$$10\log_{10}(N) = G_{dB} + 10\log_{10}(I_o) .$$

Intersecting this measured noise level with the green straight line gives:

$$G_{dB} + 10\log_{10}(I_o) = G_{dB} + 10\log_{10}(P_{IN})$$

From which we see that the input power at the point of intersection is, indeed, I_o .

Note that I_o is the received signal level that will produce 0dB SNR, i.e., signal power equal to noise power. This should not be confused with the minimum detectable power P_{MDS} which typically will be several dB lower, depending on processor settings. In the above example, a 1.2dB LOG detection threshold is shown (horizontal blue line) for the received signal. If the RVP8 is applying sufficient range and time averaging so that thermal noise alone produces very few false alarms above 1.2dB, then P_{MDS} will be a full 5dB lower than I_o. We would expect a detection rate of roughly 50% for echoes arriving at this "minimum detectable" level.

Typically a CW test signal is used to generate the test curve shown in Figure 5–10. Follow the instructions provided by the radar manufacturer for injecting a test signal. During calibration, the radar should be fully operational, so that all sources of noise are present. Ideally the transmitter should be turned on during calibration.

Important: Verify with the radar manufacturer that no damage will occur to the signal generator if the transmitter is running during the calibration.

To perform the calibration, insert signals at steps of 5 or 10 dB over the entire range of the system. Draw the plot shown in figure 5–10. You can utilize fine resolution steps at the ends of the scale to observer the details of the roll off. Be sure to raise the antenna up a few degrees to avoid ground thermal noise. Also tune the frequency of the signal generator using the setup command "pr", and displaying the received signal spectrum. Be sure to check the tuning at the end of the calibration to make sure the signal generator and IFD have not drifted apart.

Each time that a new signal level is injected, the measured power values are obtained by first invoking the SNOISE command and then reading-back the results using the GPARM command. The Log of Measured Noise Level (Word 6) from GPARM should be used. This procedure averages many samples together. For IRIS users, this is all handled by the **zauto** utility.

Finally turn it all the way down and make one more sample to measure the noise level N. I_o is obtained from the intercept of the horizontal line at N and the straight line fit to the linear portion of the curve. This value must be corrected for losses as discussed in the section below.

5.4.2 Single-Point Direct Method for Calibration of I_o

This calibration method requires no support software. The approach uses the TTY setups commands. Again the signal generator output must be calibrated in absolute dBm. Use a power meter to check the calibration.

- Turn the radiate off and connect the signal generator to the test signal injection point.
- Raise the antenna to at least 20 degrees, and set the azimuth to point away from any known RF sources including the sun.
- Select the pulse width using the mt command.
- Select the pr command and use the commands to set the following:

```
Plotting Received Power Spectrum...
Rx:Pri,  Zoom:x1–x8,  Navg:25,  Start:100.01 usec (14.99 km),  Span:50 usec
```

- Set the signal generator to the approximate radar RF frequency with a power level corresponding to a strong signal (30 dB above the noise), and use a CW signal (not a pulse). This signal should be visible as a peak in the spectrum display. Adjust the siggen RF signal frequency so that produces the precise IF frequency (e.g., IF frequency of 30 MHz).
- Turn the signal generator off and record the "Filtered" power level. Note that because of the large averaging it will require several seconds for the average to stabilize.
- Turn the signal generator on, verify that the peak is still at the IF frequency and adjust the power level to obtain precisely 3 dB more "Filtered" power than was observed with the noise only. Again, allow several seconds for the averaging to stabilize after you make each amplitude adjustment.

This is the value of I_o, i.e., the test signal signal power equals the noise power. The next step is to correct the value of I_o for losses as discussed in the section below.

5.4.3 Treatment of Losses in the Calibration

In the calibration of the dBm level of the test signal, be sure to account for any losses that may occur between the antenna feed and the injection point, and in the cable and coupler that is used to connect the signal generator to the injection point. Figure 5–11 illustrates the nomenclature of the various losses that are involved in the calibration. The relationship between the injected test signal and the value of the received power relative to the feed is:

$$dBm_{Feed} = dBm_{Injected} + dBL_{Feed:Coupler}$$

$$dBm_{Feed} = dBm_{Siggen} - dBL_{Coupler} - dBL_{Cable} + dBL_{Feed:Coupler}$$

For example, assume the following:

Loss between the feed and the coupler	$dBL_{Feed:Coupler}$	3 dB
Loss caused by the coupler	$dBL_{Coupler}$	30 dB
Loss in the cable from siggen to coupler	dBL_{Cable}	2 dB

Then if the test signal generator output is –50 dBm, the injected power is

$$dBm_{Injected} = –50–[30+2]= –82 \text{ dBm.}$$

The equivalent power at the feed is then 3 dB more than this

$$dBm_{Feed} = -82+3 = -79 \text{ dBm.}$$

During the calibration, there are several ways to handle the losses using these equations. Two examples are:

- Each signal generator value can be corrected for losses so that the calibration plot shows IFD measured power vs received power at the feed. This is recommended for manual calibration.
- The signal generator values can be plotted directly and the intercept power I_o can be corrected for losses so that it is properly referenced to power at the feed. This is the approach used by the IRIS **zauto** utility.

Figure 5–11: Illustration of Losses that Affect LOG Calibration

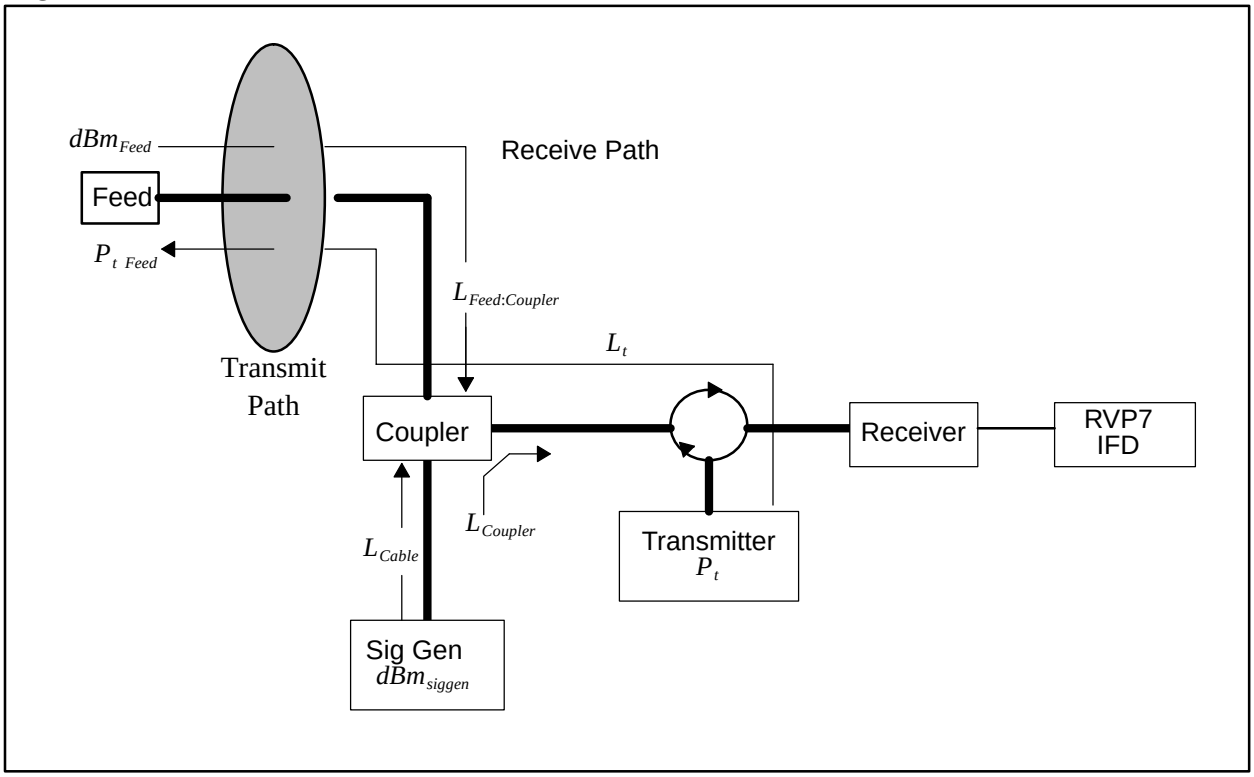

5.4.4 Determination of dBZ_o

The calibration reflectivity is determined from the radar equation as follows:

$$dBZ_o = 10 \log \left[C r_o^2 I_o \right]$$

where I_o is in mW (corrected for receive losses), the reference range r_o is 1 km, and the radar constant C is:

$$C = \frac{2.69 \times 10^{16} \lambda^2}{P_t \tau \theta \phi G^2} L_t$$

where,

λ	Radar wavelength in cm.
P_t	Transmitted peak power in kW.
L_t	Transmit loss (e.g., 3 dB corresponds to $L_t = 2$)
τ	Pulse width in microseconds.
θ	Horizontal half-power full beamwidth.
ϕ	Vertical half-power full beamwidth.
G	Antenna gain (dimensionless) on beam axis.

The radar constant is determined from the characteristics of your radar (check with the manufacturer if you are unsure of the values). Note that transmit losses are accounted for in the radar constant, while receiver loss is usually included in the calculation of I_o.

Finally, if the value of I_o calculated above was not based on loss-corrected dBm values, correct I_o as follows:

$$dBI_{o\ corrected} = dBI_o - dBL_{Coupler} - dBL_{Cable} + dBL_{Feed:Coupler}$$

Example Calculation of dBZ_o:

This sample calculation is provided so that programmers can check their arithmetic. The radar parameters:

λ	Radar wavelength in cm.	5 cm.
P_t	Transmitted power in kW.	500 kW
L_t	Transmit Loss	2 (3 dB)
τ	Pulse width in microseconds	1 microsecond
θ	Horizontal half-power beamwidth in degrees	1 degree
ϕ	Vertical half-power beamwidth in degrees	1 degree
G	Antenna gain (dimensionless) on beam axis	19,953 (43.0 dB)

The radar constant for this example is,

$$C = \frac{2.69 \times 10^{16}\lambda^2}{P_t\ \tau\ \theta\ \phi\ G^2}\ L_t = \frac{(2.69 \times 10^{16})(5)^2}{(500)(1)(1)(19,953)^2} \quad (2.0)$$
$$= 6.76 \times 10^6 \left[mm^6\ m^{-3}\ km^{-2}\ mW^{-1}\right]$$

Assume that I_o with loss correction is calculated to be –105 dBm (3.16×10^{-11} mW), then dBZ_o is,

$$dBZ_o = 10\log\left[Cr_o^2 I_o\right] = 10\log\left[\ (6.76 \times 10^6)\ (1)^2\ (3.16 \times 10^{-11})\ \right]$$
$$= -36.7dB\ (mm^6\ m^{-3})$$

This value would be down-loaded to the signal processor using the SOPRM command.

5.5 Dual PRT Processing Mode

The RVP8 supports two major modes for Dual PRT processing, i.e., algorithms using triggers that consist of alternate short and long periods. Most of the Doppler parameters are available in each of these modes. You may also request time series data in both cases; the samples will be organized so that the first pulse of a short PRT pair always comes first.

5.5.1 DPRT-1 Mode

The DPRT-1 trigger consists of a very short PRT from which Doppler data are obtained, followed by a much longer PRT whose purpose is to limit the average duty cycle of the transmitter. No information is extracted from the long PRT pair, but Dual-PRF techniques can still be used by varying the short period from ray to ray. The "-1" suffix in the name for this mode is a reminder that Doppler parameters are computed from the short PRT only. The DPRT-1 mode is intended for millimeter wavelength radars that must run at a very high effective PRF (up to 20KHz) to get an acceptable unambiguous velocity, but which also have a much lower duty cycle constraint on the average number of pulses transmitted each second.

In DPRT-1 mode the requested PRF from the host computer will generally be quite large (up to 20KHz); and the reciprocal of this "effective instantaneous PRF" will determine the trigger's short PRT interval. In this way, all subsequent physical calculations will be scaled correctly, e.g., unambiguous velocity, maximum first trip range, etc., are all supposed to be based on the short PRT interval. The host computer must therefore be configured so that it can ask for these very high trigger rates.

The duration of the long PRT interval is not specified directly by the host computer. Rather, the RVP8's "Maximum number of Pulses/Second" setup parameter is used to compute how much delay to insert in order to insure that the transmitter's duty cycle is not exceeded. This special treatment applies only in DPRT mode; all other modes that have uniform triggers continue to interpret the RVP8's trigger bound as a simple "Maximum PRF".

Since DPRT-1 mode uses only the short pairs of pulses, it is not possible to run the "R2" moment estimation algorithms. The RVP8 will return the GPARM "Invalid Processor Configuration" bit if "R2" is requested in DPRT mode. The error bit will also be returned if the number of pulses requested (sample size) is not even. All other error conditions are the same as FFT mode.

⚠ **Warning: Since the RVP8's "Maximum number of Pulses/Sec" is used to enforce the duty cycle limit, it is essential that it not be overwritten by the host computer's upper PRF limit, which typically will be much higher. To insure this, you must make sure that the PWINFO command is disabled in the RVP8 "Mc" setup menu. You will have no duty cycle protection if you do not do this.**

🛈 **Note: You may still choose to run Dual-PRF velocity unfolding within the DPRT-1 mode. What will happen is that the short PRT will vary in the selected 3:2, 4:3, or 5:4 ratio, but the overall duty cycle will remain constant. The combination of Dual–PRF and DPRT-1 is tremendously effective in extending the radar's unambiguous velocity interval.**

5.5.2 DPRT-2 Mode

The trigger consists of alternating short and long period pulses, where the ratio of the periods is determined by the velocity unfolding ratio that has been selected. Doppler data are extracted from both the short and long pulse pairs (hence the "-2" suffix), and unfolded velocities are made available on each ray based on the combined PRT data from that ray alone. DPRT-2 mode is intended for rapidly scanning radars where the ray-to-ray spatial continuity assumptions of the traditional Dual-PRF algorithms do not apply.

The DPRT-2 velocity unfolding algorithm uses a modified version of the standard Dual-PRF algorithm. Both start by computing a simple velocity difference as a first approximation of the unfolded result. The standard algorithm uses that difference to unfold the velocity from the most recent ray, which yields a lower variance estimate than the difference itself. The DPRT-2 algorithm is similar, except that the folded velocity from both PRTs are unfolded independently and then averaged together.

In addition to the above, the RVP8 also computes the DC average of the (I,Q) data within each bin. This is used as a simple estimate of clutter power, so that corrected reflectivities are available in DPRT-2 mode whenever a non-zero clutter filter is selected. DPRT-1 mode is the same in this respect. However, the DPRT-2 widths use an improved algorithm based on the two different PRTs, and which avoids the SNR sensitivity of the DPRT-1 width estimator.

5.6 Dual PRF Velocity Unfolding

For a radar of wavelength λ operating at a fixed sampling period $\tau_s = 1/PRF$, the unambiguous velocity and range intervals are given by:

$$V_u = \frac{\lambda}{4\tau_s} \quad \text{and} \quad R_u = c\,\frac{\tau_s}{2}$$

where "c" is the speed of light. Often these intervals do not fully cover the span of velocity and range that one would like to measure. The problem is generally worse for short wavelength radars, since that unambiguous velocity span is directly proportional to λ for a given τ_s. If the unambiguous range interval is made sufficiently large by increasing τ_s , then the resulting velocity span may be unacceptably small.

The RVP8 provides a built-in mechanism for extending the unambiguous velocity span by a factor of two, three, or four beyond that given above. The technique, called Dual PRF velocity unfolding, uses two pulse periods rather than one, and relies on the extra information thus obtained to correct (i.e. unfold) the mean velocity measurement from each individual period. The Dual PRF trigger pattern consists of alternating (N+k)-pulse intervals where the period in each interval is either τ_l (for the low-PRF) or τ_h (for the high-PRF). Here "N" is the sample size, and "k" represents a delay that permits the clutter filter to equilibrate to the new PRF after each change. The clutter filter impulse response lengths vary according to which filter is selected.

The two trigger periods τ_l and τ_h must be chosen in either a 3:2, 4:3, or 5:4 ratio. These ratios give factors of two, three, and four times velocity expansion over the τ_h period alone. The unfolding algorithm makes use of the following results. Suppose that the radar observes a target with mean velocity V at each of the two trigger periods. The measured phase angles for the R_1 autocorrelations at the two PRFs are:

$$\theta_l = \frac{4\pi\ V\ \tau_l}{\lambda} \quad \text{and} \quad \theta_h = \frac{4\pi\ V\ \tau_h}{\lambda}$$

where angles outside the basic $[-\pi, \pi]$ interval are returned to that interval by appropriate additions of $\pm\ 2\pi$. These angles correspond to the ordinary single-PRF Doppler velocity measurements, and the $\pm\ 2\pi$ uncertainties reflects the fact that each measurement is folded into its own unambiguous interval:

$$V_{ul} = \frac{\lambda}{4\tau_l} \quad \text{and} \quad V_{uh} = \frac{\lambda}{4\tau_h}$$

If we define ϕ to be the difference between the two measured phases then:

$$\phi = \theta_l - \theta_h = \frac{4\pi}{\lambda}\left[\tau_l - \tau_h\right]$$

which can be interpreted as a phase angle within the unfolded interval:

$$V_{u\ unfold} = \frac{\lambda}{4(\tau_l - \tau_h)}$$

Now if τ_l and figureτ_h are in a 3:2 ratio, then:

$$\tau_l - \tau_h = \frac{\tau_l}{3} = \frac{\tau_h}{2}$$

$$\text{and thus} \quad V_{u\ unfold} = 3V_{ul} = 2V_{uh}$$

The angle ϕ represents a velocity phase angle in $[-\pi, \pi]$, but with respect to an enlarged unambiguous interval. Thus, by simply differencing the folded angles from the high and low PRFs, we obtain an angle that is unfolded to a larger velocity span. Similar reasoning shows that the 4:3 ratio gives a factor of three improvement over V_{uh}.

In practice, the unfolded angle ϕ is not in itself a suitable velocity estimator. The reason is that the variance of ϕ is equal to the sum of the variances of each of its components, i.e., twice that of the individual measurements alone. If the target is at all noisy, then this increase in variance can be severe. Rather than use ϕ directly, the RVP8 uses it only as a rough estimate in determining how to unfold the individual velocity measured from each PRF.

Figure 5–12: Dual PRF Concepts

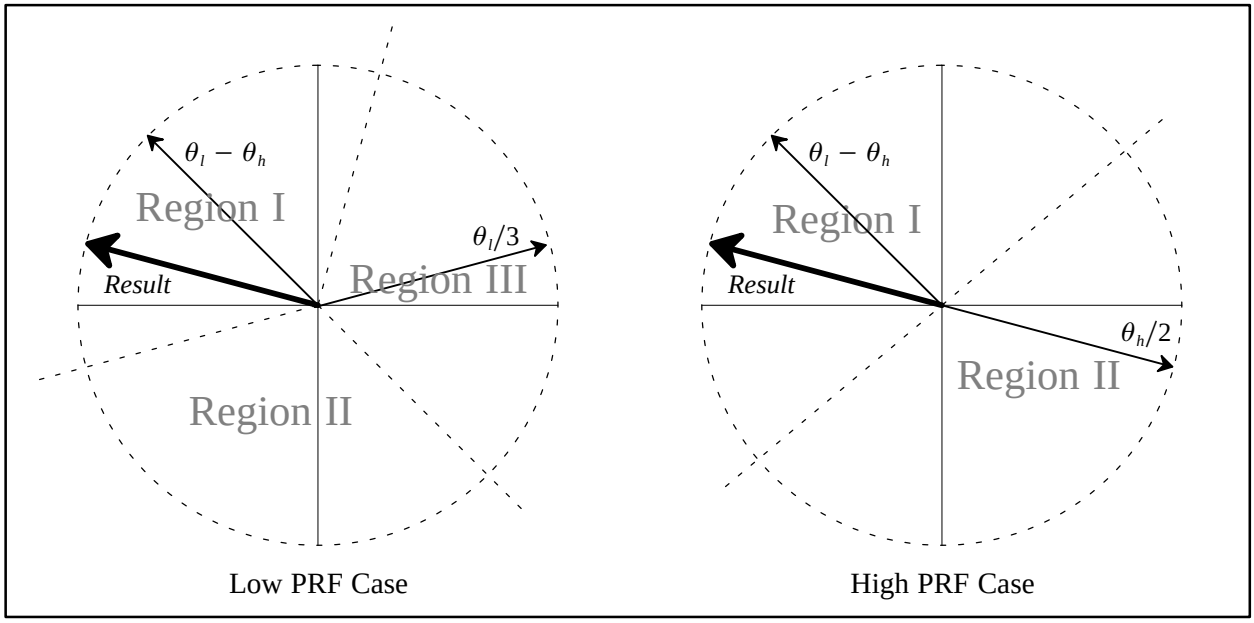

This technique is illustrated in Figure 5–12. The figure shows how the low-PRF and high-PRF angles are unfolded based on the difference angle. The diagrams show phase planes representing the large unfolded velocity interval, and the locations of various vectors on those planes. Referring first to the right figure, the difference angle is plotted, and the plane is divided into two equal size regions, one of which is centered on the difference vector. The high-PRF angle is then divided by two and plotted. The resultant unfolded velocity angle must either be this vector, or this vector plus π. Since adding π places the vector into acceptance Region 1 where it is

nearest the difference angle, we conclude that this is the correct unfolding. Likewise, on the left diagram we unfold the low-PRF angle by dividing the plane into thirds centered on the difference angle. The result angle is either

$$\frac{\theta_l}{3}\ , \qquad \frac{\theta_l}{3}+\frac{2\pi}{3} \qquad or \qquad \frac{\theta_l}{3}+\frac{4\pi}{3}$$

depending on which one falls into the acceptance Region 1. Note that the resultant angle is the same in each case.

The RVP8 makes efficient use of the incoming data by unfolding velocities from both the low and the high-PRF data, making use each time of information in the previous ray. When low-PRF data are taken the derived velocities are unfolded by combining information from the previous high-PRF interval. Likewise, when high-PRF data are acquired the velocities are unfolded based on the previous low-PRF interval. Thus, when operating in the Dual PRF mode, the RVP8 outputs one data ray for each (N+k)-pulse interval. However, the velocity data in the Dual PRF rays are unfolded, so that the [–1,+1] interval now represents either two or three times the prior velocity range. Put another way, the data are still interpreted as described in the section on mean velocity estimation, except that V_u is now larger.

The width data are also modified somewhat during Dual PRF unfolding. Although valid widths are obtained independently on all rays, those measured at low-PRF are larger than those at high-PRF. This is simply because the dimensionless width units are with respect to a larger velocity interval in the latter case. To compensate for this, low-PRF widths are multiplied by either 2/3 or 3/4 before being output. This puts them in the same scale as the high-PRF values, and thus, the widths do not vary on alternate pulses. A useful consequence of this is that width data can be sent directly to a color display generator without having to plot every other ray in a different scale.

There are a few words of caution that should be kept in mind when using the RVP8 in the Dual PRF processing modes. The unfolding algorithms make the assumption that targets are more-or-less continuous from ray to ray. Otherwise, it would not make sense to use data from a previous ray to unfold velocities in the current ray. Users must therefore assure that their antenna scan rate and beamwidth are such that each target is illuminated, at least partially, over each full 2(N+k)-pulse interval. In practice, a certain amount of decorrelation from ray to ray is acceptable, since the previous rays are used only to decide into which unfolded interval the current ray should be placed. Small errors in the previous ray data, therefore, cause no error in the output. However, large previous-ray errors would lead to incorrect unfolding.

A more subtle side effect of Dual PRF processing arises from clutter filtering because clutter notches now appear at several locations in the unfolded velocity span, rather than just at zero velocity. These additional rejection points come about because the original velocity intervals are mapped some integer number of times to create the unfolded interval. Since each original interval has a clutter notch at DC, it follows that the final expanded velocity interval will have several such notches. For example, in the 3:2 case, in addition to removing DC the clutter filter removes velocities at $-2V_u/3$, $+2V_u/3$, and V_u.

Unfortunately, these clutter filter "images" are a fundamental consequence of the Dual PRF processing technique and are not easily removed. They can cause trouble not only for the velocity unfolding itself, but because the computed clutter corrections to be wrong at the image

points. However, there is a useful work-around in the RVP8 to minimize their impact — turning the clutter filter off at far ranges where little clutter is expected and using a narrow clutter filter minimizes the effects of the clutter filter on weather targets.

The 4:3 PRF unfolding ratio is more susceptible to unfolding errors in cases where the spectrum width is large and/or the SNR is low. The user should experiment with the two ratios to determine which provides the best results for their particular application. Although the RVP8 trigger generator can produce any trigger frequency, only the 3:2 and 4:3 ratios can be used with the built-in unfolding algorithms. The RVP8 still permits other PRT ratios to be explored, but the unfolding technique must then be manually programmed on the user's host computer.

Oscilloscope observations of Dual PRF triggers can sometimes be confusing. Figure 5–13 shows seven possible scope traces (and their associated probabilities) for the RVP8 trigger during Dual PRF operation. The PRF ratio is 4:3, and the sample size is 50 pulses at the high PRF, and 37 pulses at the low PRF. The signal labelled "SCOPE" is the composite of these traces, and is what would actually be seen on an oscilloscope. Notice that there are a number of low probability pulses. The exact details of the sample sizes and the trigger hold off time can make the low probability pulses appear to come and go randomly. This is normal, and is no cause for alarm.

Figure 5–13: Example of Dual PRF Trigger Waveforms

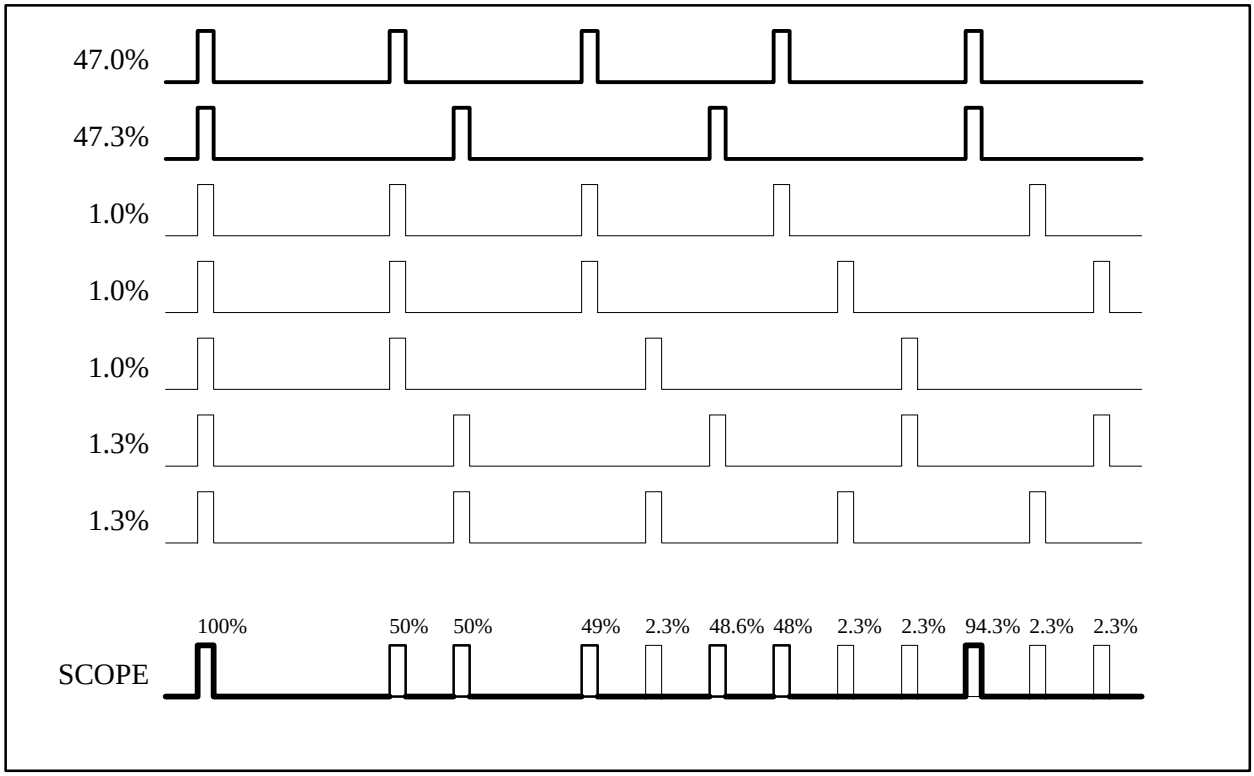

5.7 Random Phase 2nd Trip Processing

5.7.1 Overview

Second trip echoes can be a serious problem for applications when the radar is operated at high PRF (e.g., >500 Hz). Second trip echoes are caused by the range aliasing of targets. They appear as false echoes on the display, usually elongated in the radial direction. On Klystron systems they will have valid Doppler velocities. On magnetron systems, the Doppler velocities are not valid, but the noise from the 2nd trip echoes can obscure valid first trip velocity information.

The RVP8 has optional random phase processing for the filtering and recovery of second trip echoes. Details of the technique are proprietary to SIGMET, Inc. However, the general principle is described here, along with a discussion of the various configuration options to optimize the algorithm performance.

The information that is used to separate the first and second trip echoes is the phase. For a magnetron radar, the phase of each pulse is different. This means that when 1st. and 2nd trip echoes are received simultaneously, the phase of the first trip return is different from the phase of the second trip return. For a magnetron radar, the RVP8 measures the phase of the transmitted pulse and the phase locking is done digitally as opposed to the traditionally locking COHO. For a Klystron radar, the phase is controlled by the RVP8 via a digital phase shifter that is precisely calibrated. Typically the Klystron COHO is phase shifted so that each transmit pulse has a different phase. The sequencing is controlled by the RVP8.

5.7.2 Algorithm

Figure 5–14 shows a schematic of the data processing for random phase. The figure shows the Doppler spectra for the 1st. and 2nd trip in the various processing stages. The vertical scale is in dB and the horizontal scale is velocity. In this example, the second trip echo is shown as being stronger than the first trip echo (usually the reverse is true).

Ideal 1st and 2nd Trip Echoes

The ideal 1st and 2nd trip echoes represent the echoes as they would appear individually. The ideal 1st trip echo is the echo that would be measured if there were no 2nd trip echo interference. The ideal 2nd trip echo represents what would be measured if there were no 1st trip echo interference. If there is no interference from the other trip, a standard Klystron system can measure the ideal spectra, but there is no way to know whether the echoes are in the 1st or 2nd trip.

Raw 1st and 2nd Trip Echoes

This figure shows how the echoes from the first trip and second trip interfere with each other. For the case of a standard magnetron system, the first trip echo is coherent, while the second trip echo is incoherent (white noise) since the phase of the second trip echo is random. This is because the receiver is phase locked only to the first trip.

Another way to implement a magnetron system is to let the COHO free-run (rather than phase locking to the transmit pulse), measure the phase of each transmit pulse and digitally correcting for the transmit phase. Using this digital phase locking technique, the RVP8 can phase lock or "cohere" to either the first or the second trip.

Using this technique alone, it is possible to distinguish between 1st and 2nd trip echoes for the case when the echoes are not overlapped. In other words, the echoes will appear as the idealized 1st and 2nd trip echoes. This range de-aliasing effectively doubles the range of the radar. The problem is that when echoes are overlapped, the noise contamination from the stronger echo will make it impossible to measure the weaker echo. This is illustrated in the figure. Thus if the first trip echo has a good signal-to-noise ratio of 10 dB, then the 2nd trip echo will have a signal-to noise-ratio no better than –10 dB. This is the fundamental problem with using phase alone to separate the 1st and 2nd trip echoes.

Filtered 1st and 2nd Trip Echoes

Since the strong echo generates noise that obscures the weaker echo, the approach used in the RVP8 is to filter the echo from the other trip — the whitening filter. This is shown in the figure. The adaptive whitening filter removes both the clutter and the weather. All of the phase information for the other trip is then contained in the white noise portion of the spectrum. Note that the phase information under the coherent echo that is removed will be dominated by the coherent echo, i.e., the other trip phase information will be contaminated. For this reason, the filtering should effect as small a region of the spectrum as possible.

5.7.3 Tuning for Optimal Performance

The Random Phase algorithms are controlled by the same collection of setup and operational parameters that apply to all of the other processing modes, e.g., choice of sample size, clutter filter, angle sync, calibration, etc. However, a few parameters are special to Random Phase mode, and these are described below.

Secondary SQI Threshold

In standard Doppler processing, an SQI threshold is normally not applied to Reflectivity data because it would cause those data to be rejected in regions of high spectral width. In Random Phase mode we need to relax this convention because reflected power can only be assigned to a particular trip when it is coherent within that trip. Incoherent echoes, regardless of their strength, can not be placed into either trip.

Thus, an SQI threshold is required to qualify Reflectivity data in Random Phase mode. The RVP8 defines a secondary SQI threshold SQI_2 which is computed from the standard threshold value simply as:

$$SQI_2 = Offset + (Slope \times SQI)$$

Where *Slope* and *Offset* are the Random Phase SQI threshold parameters defined in the **Mf** setup section. The factory default values are $(Slope = 0.50)$ and $(Offset = -0.05)$, i.e., the secondary threshold is a little less than half of the standard value. The Random Phase

algorithms check whether the SQI of each recovered trip is less than the secondary SQI threshold, and if so, the LOG portion of the data are rejected. This SQI test is necessary for a clean LOG picture, but we need to use a more permissive (lower) threshold value than would usually be applied to the Doppler data alone.

The *Slope* and *Offset* values should be adjusted so that the density of speckles in Random Phase LOG data is approximately the same as the density of speckles in FFT velocity data for a given primary SQI value. You may then adjust the primary SQI threshold to achieve the appropriate tradeoff of speckles vs. sensitivity for your system in all modes of operation. Even with proper adjustment, it is normal for Random Phase *dBZ* and *dBT* data to show "holes" in regions of weather that have high turbulence or shear. These dropouts will usually match up with similar gaps in the velocity and width data, both of which are traditionally thresholded by SQI.

Maximum Power Ratio Between Trips

The adaptive filtering that is performed on the data for each trip greatly extends the visibility of a weak echo that is overlapped with a much stronger one. In practice, the filtering process is often able to remove 25-35dB of dominant power in order to reveal a much weaker echo in the other trip. The performance depends on many factors, primarily the spectral width of the dominant echo, and the overall stability of the radar system.

The difficulties of removing a dominant "other trip" echo from a weather signal are analogous to the challenge of removing a dominant clutter target from that same signal. In both cases we are trying to extract a weak weather signature using a filtering procedure that relies on the spectral confinement of the stronger signal. The RVP8 already has a parameter that can be adjusted to control sub-clutter visibility, i.e., the Clutter-to-Signal Ratio (CSR). Just as the CSR applies to the clutter filters, it can likewise be used to place similar limits on the depth of visibility of the adaptive filters.

As an example, suppose that the RVP8 is operating in Random Phase mode at a PRF of 1500Hz, and is observing widespread weather having uniform intensity in both the first 100Km trip and the second 100Km trip. If the CSR were set too conservatively at only 15dB, then the algorithm would generally be blind to second-trip weather in the range interval from 100km to 117.8km. The explanation for this can be found in the $1/r^2$ geometric correction for weather echo intensity. At ranges less than 17.8km, the first trip weather would generally dominate the second trip weather by more than 15dB. Thus, the initial 17.8km ring of second trip data would be rejected by the CSR criteria. However, if the CSR were increased to 30dB, then the size of this missing ring would be reduced to only 3.2km.

If the CSR is set too low you will notice an abrupt ring of missing data in the beginning of the second trip. If set too high, there will be speckles and other spurious effects within this same interval. The optimum setting should strike a balance between these two effects.

R1 vs. R2 Algorithms

The Random Phase algorithms for adaptive filtering and separation of trips relies on having the best possible information about the weather's SNR and spectral width. Thus, the "R2" Doppler algorithms are always used, regardless of the setting of the R1/R2 flag in the user's operational parameters.

Random Phase and Dual PRF

The random phase processing works seamlessly with the dual PRF processing to provide advanced range and velocity ambiguity resolution. Both the first and 2nd trip echoes can be recovered and displayed to a maximum range of 2X the unambiguous range corresponding to the high PRF.

For optimum performance, the 2D 3x3 speckle filter should be used to smooth the 2nd trip seams that occur for each ray. In fact, this smoothing of the 2nd trip seam makes the dual PRF random phase mode work even better than the single PRF random phase.

Figure 5–14: Random Phase Processing Algorithm

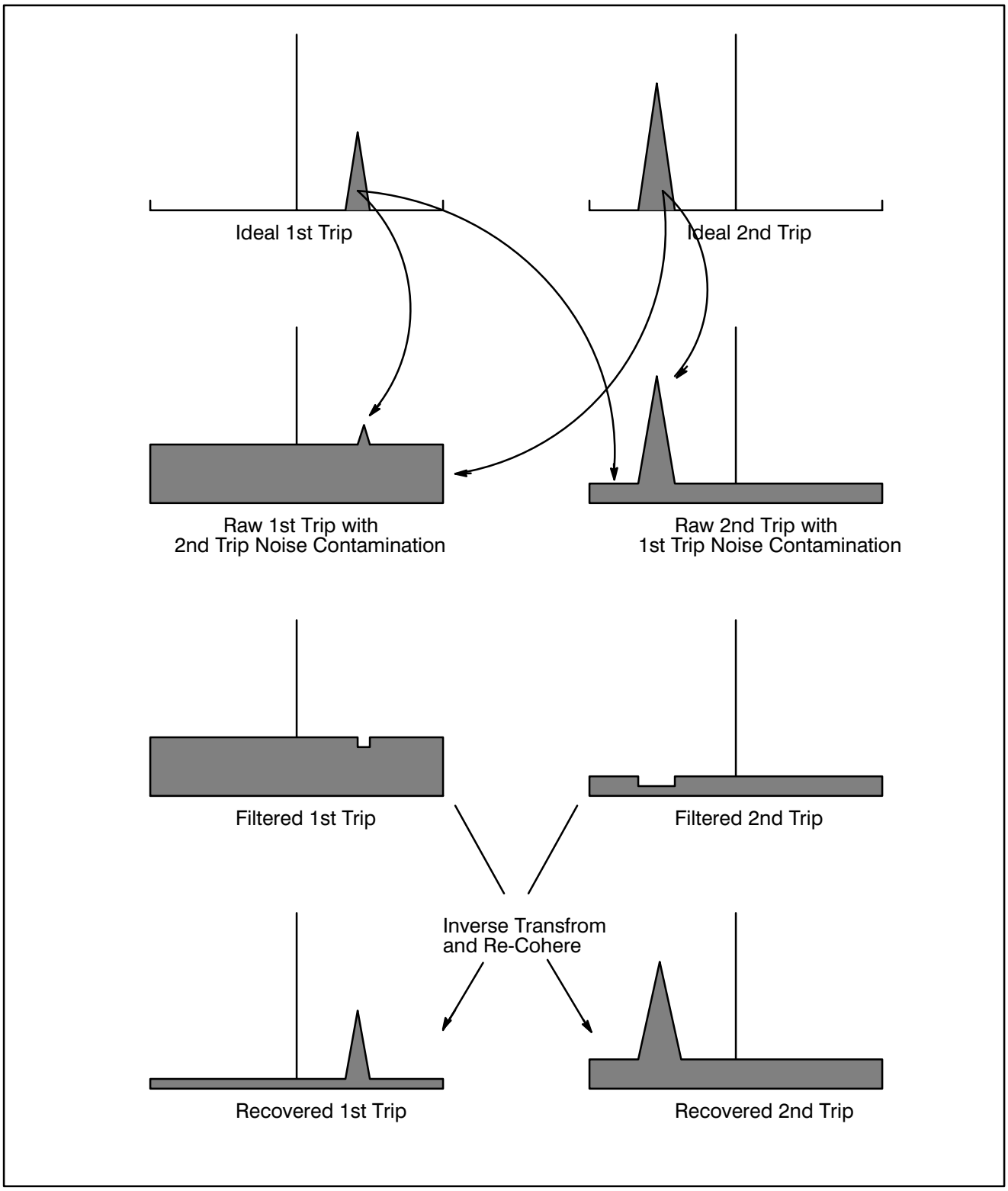

5.8 Signal Generator Testing of the Algorithms

This section describes a variety of IF signal generator tests that can be used to verify correctness of the RVP8 processing algorithms. These tests are routinely performed at SIGMET whenever new algorithms and/or major modes are added to the processor. We have include a few of the test descriptions here so that they can be used by customers who need to debug their systems, or who want to better understand how they work. Additional tests for receiver sensitivity and dynamic range can be found in Appendix D.

5.8.1 Linear Ramp of Velocity with Range

Suppose that a continuous-wave IF waveform has an instantaneous frequency $f(t)$ in Hertz (cycles/sec). Consider a range bin located at time τ_{bin} within a set of pulses that are separated by $\tau_s = 1/PRF$. The phase measured at that bin on the n^{th} pulse will be the integral of the frequency within that pulse starting from range zero (since the RVP8 is phase locked to range zero):

$$\Phi_n = \int_{n\tau_s}^{n\tau_s+\tau_{bin}} f(t)dt$$

If we assume that the input frequency is a linear Frequency Modulation (FM) at the rate of M cycles/sec/sec on top of a base frequency T_o, then:

$$\Phi_{n+1} - \Phi_n = \int_{(n+1)\tau_s}^{(n+1)\tau_s+\tau_{bin}} (T_o + Mt)dt - \int_{n\tau_s}^{n\tau_s+\tau_{bin}} (T_o + Mt)dt = (M\tau_s)\tau_{bin}$$

which, remarkably, is independent of both T_o and n. Thus, a linear FM input signal produces a fixed (I,Q) phase difference from pulse-to-pulse at any given range. The magnitude of the phase difference is proportional to the range, and the slope is $(M\tau_s)$ cycles for each second of delay in range. For example, if the test signal generator is sweeping 100KHz every two seconds, then the velocity observed at a range of 300km at 250Hz PRF will be:

$$\Phi_{n+1} - \Phi_n = \left(\frac{100\ KHz}{2\ \text{sec}}\right) \times \left(\frac{1}{250}\text{sec}\right) \times (300\ km) \times \left(\frac{6.6\ \mu\ \text{sec}}{1\ km}\right) = 0.40\ cycles$$

We would thus observe a velocity of $(0.8 \times V_u)$ at 300km, where V_u is the unambiguous Doppler velocity in meters/sec. Note that these phase difference calculations have made no assumptions about the RVP8 processing mode, and thus are valid in all major modes (PPP, FFT, DPRT, RPH), as well as in all Dual-PRF unfolding modes.

Interestingly, this simple FM signal generator will also produce valid second trip velocities that can be seen during Random Phase processing. This follows from the above analysis because we've never assumed that τ_{bin} was smaller than τ_s, i.e., it is fine for the range bin to be located in any higher-order trip.

5.8.2 Verifying PHIDP and KDP

The PHIDP and KDP processing algorithms can be tested using CW signal sources at IF. In the alternating-transmitter single-receiver case, a single FM signal generator is modulated with an RVP8 polarization select line so that slightly different frequencies are generated for the H and V pulses. A maximum FM depth of several kilohertz is all that is required. In the dual-receiver case, two (unmodulated) signal generators are used for each of the H and V intermediate frequencies, and one or the other is detuned slightly from its correct center frequency. In either case the frequency difference that produces a KDP value of 1.0 degree/km will be:

$$\left(\ 1.0 \ \frac{degree}{km} \ \right) \times \left(\ \frac{1}{360} \ \frac{cycles}{degree} \ \right) \times \left(\ 299792 \ \frac{km}{second} \ \right) \ = \ 833 \frac{cycles}{second}$$

5.8.3 Verifying RHOH, RHOV, and RHOHV

These three terms measure the normalized cross-channel covariance in a polarization radar. They all are computed in essentially the same way having the form:

$$RHOAB \ = \ \frac{< \ s_A^n \ s_B^{n\,*} >}{\sqrt{< \ s_A^2 \ >< \ s_B^2 \ >}}$$

Where the s_A^n and s_B^n are complex (I,Q) vectors from two receiver channels A and B, and "<>" denotes expected value. This suggests that some form of amplitude modulation (AM) of the input signal might be helpful.

Suppose that the s_A^n and s_B^n samples are coming from two signal generators installed on a dual-receiver system, and that only the B-Channel is AM modulated so that:

$$| \, s_A^n \, | \ = \ \{ \, S_A, S_A, S_A, S_A, S_a \ \ldots \, \} \ \ , \ \ | \, s_B^n \, | \ = \ \{ \, S_B, 0 \, , S_B, 0 \, , S_B \ \ldots \, \}$$

Then the above estimator reduces to:

$$RHOAB \ = \ \frac{(\frac{1}{2}) \, S_A \, S_B}{\sqrt{S_A^2 \times (\frac{1}{2}) \, S_B^2}} \ = \ = \ 0.707$$

A simple way to create these data is to set the A-Channel siggen for 95% AM depth, and use a sinusoidal modulation source of, perhaps, 400Hz. The reason for not choosing 100% depth is that we would loose the Burst phase reference when the amplitude became smallest. The 26dB reduction in S_B is a close enough approximation to zero in the above formula.

If we now observe the two receive channels with the RVP8 at a PRF of 800Hz, we will see the various RHOAB terms varying with range; reaching a high value of 1.00, and a low value of 0.707. The plots will be nearly stationary on the **ascope** screen because the PRF is almost precisely twice the modulation rate (though they are free-running relative to each other).

Adjusting the amplitude of either signal generator will not affect the ρ terms, but it will have an interesting effect on SQI. If (T,Z,V,W) are being computed from both channels combined, then the SQI is:

$$SQI \ = \ \frac{S_A^2}{S_A^2 \ + \ (\frac{1}{2}) \, S_B^2}$$

If we solve this equation for SQI=0.5 we find that the individual S_A terms must have twice the power of the individual S_B terms. This can be checked by adjusting either signal generator until the minimum plotted SQI is 0.5, and then verifying that the average *H* and *V* powers are identical; or, equivalently, that *ZDR, LDRH* and *LDRV* are zero.

The linear FM ramp described in Section 5.8.1 can also be used as a test of RHOAB in a dual-receiver system. With one siggen modulated and the other fixed, one receive channel will appear to be rotating relative to the other. If the FM modulation is such that *1/N* of a full revolution occurs per pulse at a given range, then if the sample size is *N* pulses we will observe $RHOAB = 0$ at that range. In fact, the plot of *RHOAB* will show a characteristic $sin(x)/x$ behavior as a function of range.